

Graphene and CNT-Based Smart Fiber-Reinforced Composites: A Review

Mohammad Hamidul Islam, Shaila Afroj, Mohammad Abbas Uddin, Daria V. Andreeva, Kostya S Novoselov, and Nazmul Karim*

Multifunctional fiber-reinforced polymer (FRP) composites provide an ideal platform for next-generation smart composites applications including structural health monitoring, electrical and thermal conductivity, energy storage and harvesting, and electromagnetic interference shielding without compromising their mechanical properties. Recent progress in carbon-based nanomaterials such as graphene and carbon nanotubes (CNTs) has enabled the development of many novel multifunctional composites with excellent mechanical, electrical, and thermal properties. However, the effective incorporation of such carbon nanomaterials into FRP composites using scalable, high-speed, and cost-effective manufacturing without compromising their performance is challenging. This review summarizes the recent progress on graphene and CNT-based FRP composites, their manufacturing techniques, and their applications in smart composites. Current technical challenges and future perspectives on smart FRP composites research to facilitate an essential step toward moving from research and development-based smart composites to industrial-scale mass production are also discussed.

1. Introduction

Smart fiber-reinforced polymer (FRP) composites, comprised of a polymer matrix reinforced with fibers and functional materials, can reversibly change their properties with changing environmental stimuli, including mechanical, chemical, electrical, light, temperature and moisture, and can be used as chemical and strain sensors, energy harvesters and storage device, actuators, switches, robots, artificial muscles, and controlled drug delivery.^[1] Such composites are usually based on functional metal alloys, inorganic compounds, polymers, and carbon nanomaterials.^[2–4] Among them, carbon-based nanomaterials have drawn significant interest in developing high-performance smart composites.^[5–8]

Carbon-based nanomaterials such as graphene and carbon nanotube (CNT) are attractive components for smart and multi-functional FRP composites applications because of their excellent mechanical, electrical, optical, and thermal properties.^[1] For example, CNT is a 1D tube that demonstrates a high aspect ratio ranging from 30 to 1000.^[9] Thus, it has drawn significant interest as reinforcement fillers to develop superior composites with enhanced mechanical and physical properties.^[10] In addition, the isolation of graphene in 2004^[11] has unveiled some novel 2D materials and their derivatives with excellent mechanical and multi-functional properties.^[12–16] Such materials have shown great promise for use in structural composites applications due to their outstanding mechanical properties.^[17–21] Furthermore, 2D materials can be produced in uniform dispersions via scalable, low-cost, and mass production methods^[22] with great potential for applications in electronics, energy, membranes, coatings, and composites.^[13,21,23] Graphene-based smart composites hold specific promise due to their advantage over other carbon allotropes to develop next-generation multifunctional and structural FRP composites.^[24]

The uses of CNT in polymer composites started in early 1990 when CNT was reported for the first time in the scientific literature.^[25] The use of CNT in FRP composites was found in early 2000^[7] and plays a significant role in improving the structural and non-structural functionalities.^[26] The research and patenting activities on graphene-based polymer composite have increased greatly since its isolation.^[8] Significant efforts

M. H. Islam, S. Afroj, N. Karim
Centre for Print Research (CFPR)
The University of the West of England
Bristol BS16 1QY, UK
E-mail: nazmul.karim@uwe.ac.uk

M. A. Uddin
Department of Dyes and Chemicals Engineering
Bangladesh University of Textiles
Tejgaon, Dhaka 1208, Bangladesh

D. V. Andreeva, K. S. Novoselov
Department of Materials Science and Engineering
National University of Singapore
Singapore 117575, Singapore

K. S. Novoselov
Institute for Functional Intelligent Materials
National University of Singapore
Singapore 117575, Singapore

K. S. Novoselov
Chongqing 2D Materials Institute
Liangjiang New Area, Chongqing 400714, P. R. China

 The ORCID identification number(s) for the author(s) of this article can be found under <https://doi.org/10.1002/adfm.202205723>.

© 2022 The Authors. Advanced Functional Materials published by Wiley-VCH GmbH. This is an open access article under the terms of the Creative Commons Attribution License, which permits use, distribution and reproduction in any medium, provided the original work is properly cited.

DOI: 10.1002/adfm.202205723

have been made to improve the mechanical and functional properties of FRP composites by using such nanomaterials. In nanomaterials-based FRP composite, three different materials coexist: macro-scale reinforcement (fiber), nano-scale reinforcement (CNT, graphene), and polymer matrix.^[27–29] There are mainly two approaches that have been used to incorporate graphene and CNT in the FRP composites, either through dispersing nanomaterials into the matrix (i.e., matrix modification)^[30] or applying nanomaterials to reinforcement materials (i.e., reinforcement modification).^[31]

Graphene and CNT-based smart composites have been studied intensively in recent years with various nanomaterial

incorporation techniques and composite manufacturing methods.^[8,32–35] There exist reviews on graphene reinforced,^[32] CNT reinforced,^[33] graphene-based glass and carbon fiber (CF) reinforced,^[8] CNT-based CF reinforced,^[34] graphene-based CF reinforced,^[35] and graphene incorporated natural fiber reinforced^[36] composites. However, there is a lack of a comprehensive review that covers the manufacturing process, mechanical and functional properties, and applications of both graphene and CNT-enhanced synthetic and natural fiber reinforced smart FRP composites. In this review, we summarize advances in the preparation of CNT and graphene-based smart FRP composites. We also discuss the reinforcement and matrix

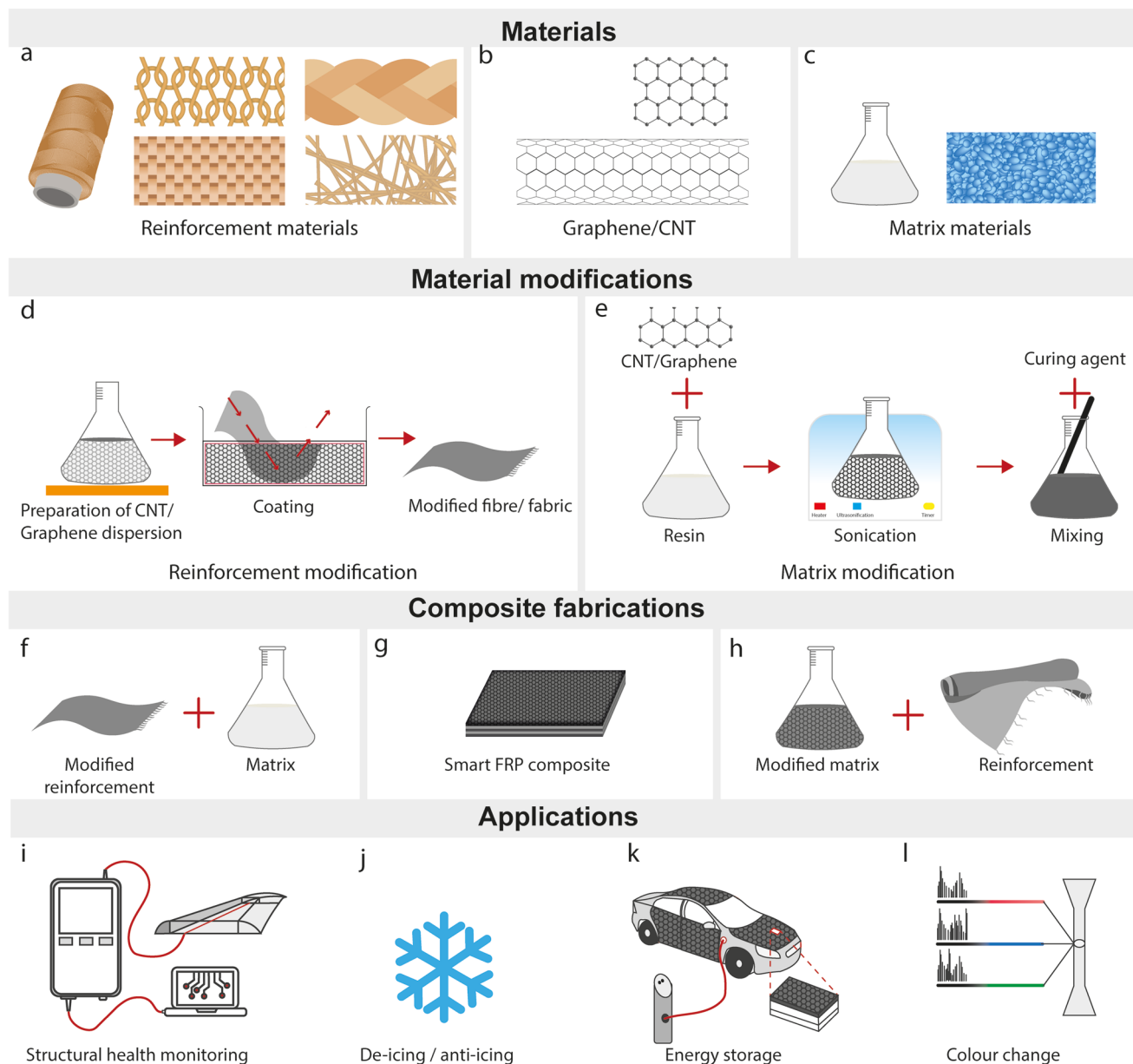


Figure 1. Schematic illustration of the outline for this review. Raw materials needed to produce smart composites: a) reinforcement materials, b) nanomaterials and c) matrix materials. Material modifications with carbon-based nanomaterials: d) reinforcement modification and e) matrix modification. Manufacturing of smart FRP composite: f) from modified reinforcement, g) smart FRP composite, and h) from modified matrix. Potential applications of smart composites: i) structural health monitoring, j) de-icing/anti-icing, k) energy storage, and l) color change.

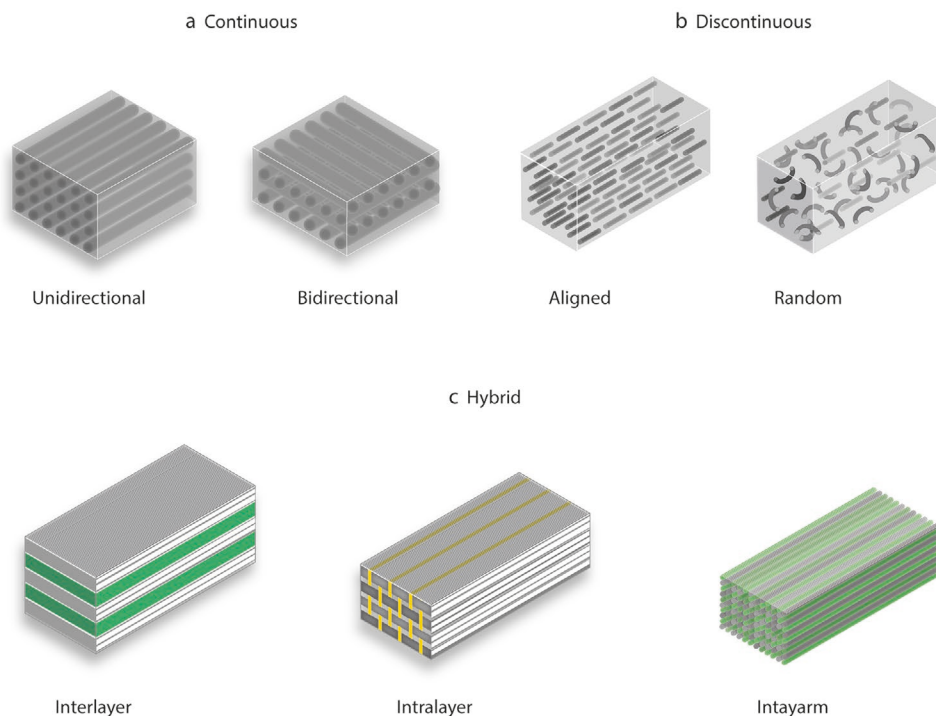


Figure 2. Schematic illustrations for FRP composites: a) continuous FRP composites: unidirectional and bidirectional arrangements of fibers, b) discontinuous FRP composites: aligned and random arrangements of fibers, c) hybrid composites: Interlayer, Intralayer, and intra-yarn arrangement.

modifications with graphene and CNT, and the fabrication and manufacturing techniques of smart composites. We then focus on applications of such composites in structural health monitoring (SHM), de-icing/anti-icing, energy storage, and color-changing composites, followed by the challenges that must be overcome for these composites to be adopted in practical applications. A Schematic illustration of the outline for this review is presented in **Figure 1**.

2. Basic Principles of FRP Composites

2.1. Structure of FRP Composites

The structure of FRP composites consists of mainly two components: fiber and polymer matrix. The fiber can be used at different scales and in various forms such as filaments, tows, yarns, woven, knitted, or braided fabrics, and mats. According to

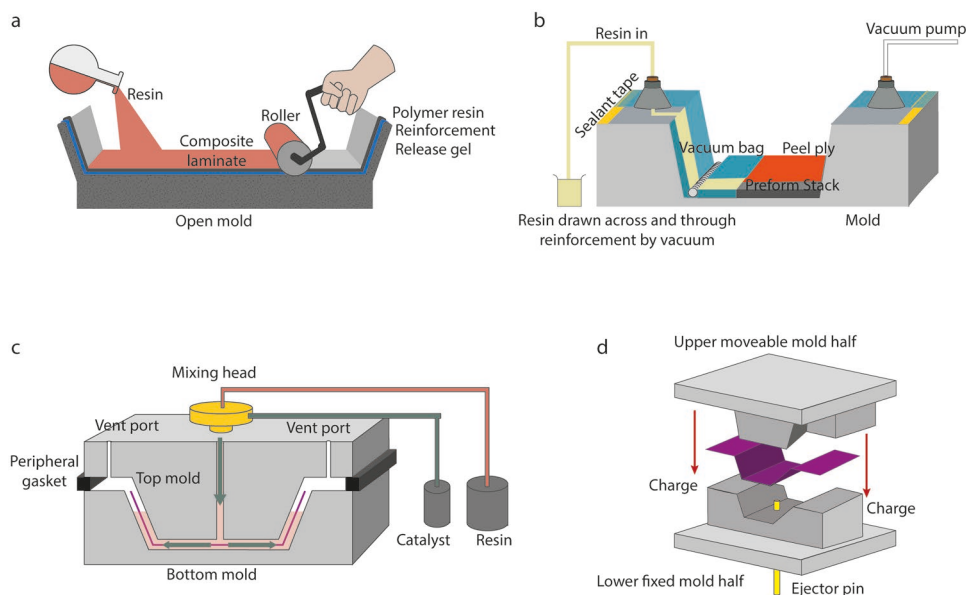


Figure 3. Schematic illustrations of FRP composites manufacturing methods: a) hand lay-up, b) vacuum-assisted resin infusion, c) resin transfer molding, and d) compression molding method.

the length of the reinforced fibers in the composite, they can be classified as continuous and discontinuous FRP composites.^[37] Composite with long fiber reinforcements is called a continuous FRP composite (Figure 2a), and that with short fiber reinforcements is called a discontinuous FRP composite (Figure 2b). In the continuous FRP composites, the fiber can be placed unidirectionally (UD) or bidirectionally. For discontinuous FRP composite, the fiber can be arranged randomly or aligned in the composites structure. Another type of FRP composite is called hybrid composites (Figure 2c). Hybrid FRP composites are manufactured from two or more fiber types in a single matrix structure. According to the arrangement of the fibers in the composite, hybrid composites can be categorized into three major types: interlayer or layer by layer, intralayer or yarn-by-yarn, and intra-yarn or fiber-by-fiber.^[38] The mechanical and structural properties of the composites depend on the arrangement of fibers in the composite structure. The fibers used as reinforcement materials are either synthetic (carbon, glass, aramid, etc.) or natural (jute, flax, ramie, coir, etc.); whereas matrix materials used are either thermoset (polyester, epoxy, vinyl ester, phenolic, etc.) or thermoplastic (polypropylene, polyethylene polycarbonate, etc.) resins. Fibers are inherently stronger than the matrix, which contributes to the strength and stiffness of composite materials. The polymer matrix works as a binder to hold fibers together and transfers the load to reinforcement fibers when the load is applied and distributes the stress among the fibers. Therefore, the presence of appropriate interfacial bondings between fiber and matrix is important for effective stress transfer from weaker matrix to stronger fiber.^[39,40] The strength of interfacial bondings between the fiber and matrix depends on mechanical interlocking, intermolecular interactions, chemical bonds, and the phase separation phenomenon.^[34,41] The mechanical properties of the FRP composites depend strongly on the properties of the reinforced fibers, matrix, and the physical or chemical properties at their interface.^[42] The major challenge is the fabrication of FRP composites with enhanced fiber-matrix interfacial bonding for effective stress transfer.

Over the last few decades, extensive research has been undertaken to improve fiber-matrix adhesion.^[39,43,44] In such cases, different physical and chemical approaches have been investigated to modify either reinforcing fibers, polymer matrices, or both fibers and matrices. Several techniques have been used to modify reinforcement fibers, including physical treatments (such as plasma, UV, and heat treatment),^[45–47] chemical treatments,^[48] and coating with nanomaterials (such as graphene and CNT). In addition, the modification of polymer matrices with nanomaterials has been widely used. Recent studies have demonstrated that nanomaterials (graphene and CNT) based modifications of fibers and polymer matrices offer a significant improvement in mechanical and interfacial properties of FRP composites.^[8,49–56] Complementary to these, the incorporation of carbon-based nanomaterials to FRP composites also adds new functionalities such as sensing, SHM system, electrical and thermal conductivity, and energy storage.

2.2. Manufacturing Techniques

FRP composites are usually manufactured via a combination of fibers and polymer matrices. Many manufacturing

techniques are available to fabricate FRP composites: hand lay-up,^[57] vacuum-assisted resin infusion (VARI),^[58,59] resin transfer molding,^[60,61] vacuum-assisted resin transfer molding (VARTM),^[62,63] pre-impregnated (prepreg) form,^[64] filament winding,^[65] pultrusion,^[66] compression molding,^[67] and automated fiber placement (AFP).^[68] The choice of manufacturing technique depends on the component size, geometry, desired mechanical properties, and the scale of production.

Hand Lay-up: Hand lay-up is the most commonly used FRP composites manufacturing technique, usually used to manufacture thermoset composites (Figure 3a). It is a simple and open molding method, where reinforcement fibers are placed on one side of the mold by hand, and then the resin is applied with a brush or roller. The excessive resins and entrapped air are removed manually with a roller. Usually, the curing process is carried out at room temperature. This is a low-cost composite manufacturing technique due to less capital cost. However, the product quality depends largely on the operator's skills. In addition, there is a possibility of producing inconsistent products with low fiber volume fraction (V_f) in the composites.

Vacuum-Assisted Resin Infusion: VARI is an improved version of the hand lay-up method. An important step is to evacuate the air from reinforcement fibers before infusing the resin. Once the vacuum process is completed, the resin is carefully sucked into the laminate through the resin inlet and outlet tube. Thermoset resins are usually used in this method of composite manufacturing. VARI process provides better V_f (i.e., fiber-to resin ratio), therefore producing stronger FRP composites than the hand lay-up method. Such a manufacturing process is cost-effective for large structural components and eco-friendly as the fabrication process is carried out inside a vacuum bag (Figure 3b).

Resin Transfer Molding: RTM method is generally used to make good surface finished composites at high temperatures. In this process, reinforcement materials (preforms) are placed in the mold first, then closed and clamped. After that, the thermoset polymer matrix is injected into the mold under pressure, and the component is cured inside the mold (Figure 3c). The resulting composites from such a process have a very smooth and high-quality surface finish on both sides and contain much less void. The RTM process has a moderate to higher production rate and the ability to produce complex-shaped composites.

Compression Molding: Compression molding is another method used for manufacturing both thermoset and thermoplastic polymer composites. The feeding materials are placed into an open pre-heated mold cavity during this process. The mold is then closed with a top plug and compressed with large hydraulic pressure (Figure 3d). Then the required pressure and temperature are applied to cure (for thermoset) or consolidate (for thermoplastic) the materials. Once the process cycle is finished, the composite part is removed from the mold. The process is expensive because of the higher mold and equipment cost.

Autoclave Molding: Autoclave molding is a commonly used technique, similar to vacuum bagging but with few changes, such as the layup is being subjected to greater pressure.^[69] Such a method is widely used in the aerospace industry for the pro-

duction of high-quality prepreg-based parts. Prepregs are composite materials where a thermoset or thermoplastic polymer matrix material with a suitable catalyst is added to reinforcement fibers at a certain ratio. The polymer matrix in prepregs is then partially cured and stored in a cool place (at ≈ 4 °C) to avoid complete polymerization.^[70] To manufacture composites, the prepregs are placed on a mold, similar to the hand lay-up method. The prepregs are then covered with a vacuum bag to remove the air. Finally, the prepregs are cured in an autoclave according to a specific pressure and temperature cycle.^[71] Such a process can provide higher V_f due to the accurate matrix content in the prepreg set by the manufacturer. This process could be automated to save labor costs. However, it is currently an expensive process due to the requirements of higher curing temperature, and expensive materials and equipment (autoclave) costs.

Automated Fiber Placement: AFP is an advanced composite manufacturing technique used to fabricate multi-stiffened laminated composites.^[72] The AFP process involves various phases of design, process planning, manufacturing, and inspection. AFP is a hybrid process where filament winding and automated tape laying can be used. Both flat and cylindrical structures can be manufactured using this method. There are three main types of materials used for AFP methods: thermoset prepreg, thermoplastic prepreg, and dry fiber. Multiple tows or roving with narrower widths can be used in this technique. Tows are pulled off from spools and fed into a fiber placement head through a delivery system. The fiber placement head follows the program to place the fiber directly onto a tool or work surface to create a preform. Advantages of this process are automation, low material wastage, and repeatability of manufacture. However, the cost of processing equipment is high.

2.3. Metrics for Smart FRP Composites Performances

Smart FRP composites have recently seen significant scientific and technological developments for producing next-generation multifunctional materials. Smart composites have exclusive structural, processing, and sensing abilities. Such composites have outstanding mechanical properties and possess multifunctionalities such as SHM, electrical and thermal conductivity, energy storage and harvesting, and electromagnetic interference (EMI) shielding. In a smart FRP composite, fiber and matrix elements ensure the load-bearing capability, and functional materials offer multi functionalities.^[73] Over the past decade, graphene and CNT have been used to manufacture smart FRP composites. The amount and distribution of such functional nanomaterials can be controlled in the composite structure according to the desired properties. The advantages of such materials are their light weight and smaller size with higher mechanical properties, and less expensive and easy process to integrate such materials within a composite structure.

It is necessary to characterize and measure physical properties of all constituents, desired functionalities, and the mechanical and environmental behavior of smart FRP composites. Many techniques can be applied for the characterization of graphene and CNT-based smart FRP composites, such as measurement of strength and stiffness, interfacial properties, electrical conductivity,^[75] thermal conductivity,^[76] EMI shielding,^[77]

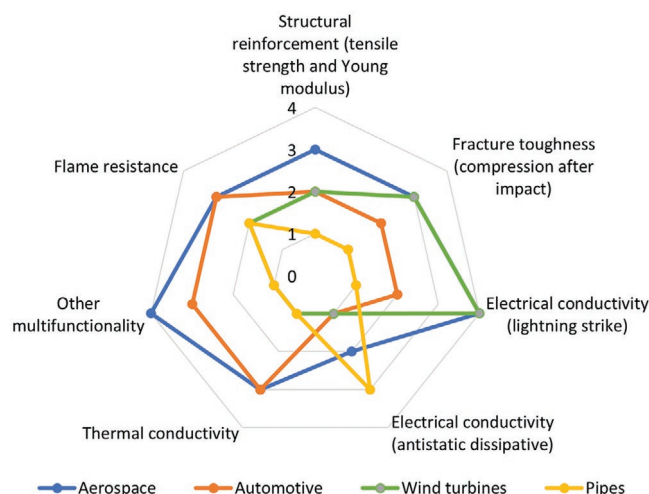


Figure 4. A radar chart comparing smart composite performance for various applications. Reproduced with permission.^[74] Copyright 2019, Elsevier Limited.

SHM,^[78] acoustic emissions,^[79] in situ damage sensing,^[80] and flame resistance. **Figure 4** shows a radar chart that compares smart composite performances for various applications. The multifunctionalities of FRP composites can vary in type and intensity for different applications. For example, a lightning strike is a major problem for composite materials used in aerospace and wind turbines.^[81] Incorporating electrical conductivity in composite materials is important to improve the resistance to lightning damage. Additionally, piezo-resistive damage sensing and energy storage for power distribution in all body parts of modern cars and airplanes are desirable.^[82] Furthermore, ice accumulation on aircraft wings and wind turbine blades is often an issue for FRP composites. By increasing the thermal conductivity of FRP composites, anti- and de-icing structures can be developed to solve such problems.^[83] FRP composites pipes are used in the oil/gas, buried water pipe, and chemical industries, as they show better chemical resistance than metals. Antistatic electrical conductivity and flame resistance properties are desired for such applications.^[84]

3. Carbon Materials and Their Production

3.1. Graphene and Its Derivatives

Graphene has received significant interest from the research community due to its remarkable mechanical, electrical, and thermal properties, which are interesting for both blue sky and application-based research. The fundamental requirement for successful commercial applications of such materials is highly scalable, reliable, and cost-effective production processes. The graphene production methods can broadly be categorized into top-down and bottom-up techniques. In top-down techniques, graphene is mainly exfoliated from the bulk graphite.^[85] The benefit of such a process is solution-based processability, ease of implementation, and higher yield compared to a bottom-up process.^[86] In contrast, graphene flakes are deposited on a suitable substrate from carbon sources in bottom-up techniques.

Chemical vapor deposition (CVD),^[87] Plasma enhanced CVD,^[88] and epitaxial growth of graphene on silicon carbide (SiC) substrate^[86] are commonly used bottom-up techniques. The benefit of such a technique is the production of contamination-free graphene with control over the initiation and growth of graphene via the correct choice of substrate. However, bottom-up methods are not very popular for large-scale production due to their low yield, complex processing, and associated higher cost.^[86]

Among several graphene exfoliation methods, the liquid phase exfoliation (LPE) processes are widely used due to their versatility, scalability, simplicity, and cost-effectiveness.^[89] In LPE processes (Figure 5a), ultrasonic or shear energy is applied to break inter-sheet forces of carbon in the presence of a stabilizer (e.g., urea),^[90,91] either in a non-aqueous solution^[90,92–95] or an aqueous solution with surfactant.^[90,93] The flake size of graphene produced via LPE is mostly below $1 \mu\text{m}^2$, possibly due to in-plane fracture during the exfoliation and purification process of separating unexfoliated flakes.^[90,94–97] Among other LPE processes, microfluidic exfoliation is a recent approach for exfoliating graphene,^[98] which was a very well-established technique for manufacturing polymer nanosuspensions,^[99] liposome nanoparticles,^[100] aspirin nanoemulsions,^[101] oil-in-water nanoemulsions,^[102] de-agglomerating and dispersing carbon nanotubes.^[103] It is a homogenization technique where high pressure (up to 207 MPa)^[103] is applied, which forces the whole volume of liquid to pass through a Z-shaped microchannel (diameter, $d < 100 \mu\text{m}$), (Figure 5b). Therefore the force acts over the full volume of the liquid; and thus achieves 100% yield by weight (Y_w)^[104] and a higher concentration compared to other LPE processes as the force acts over the whole volume of the liquid. However, other LPEs method such as bath sonication, tip sonication, and shear exfoliation generally produce graphene with concentrations as low as 0.1–0.2,^[94] 0.2,^[105,106] and $<0.1 \text{ g L}^{-1}$,^[99,107] consecutively, and yield by weight (Y_w) as

low as $\approx 1\text{--}2\%$,^[94] 1% ,^[105,106] and $2 \times 10^{-3}\%$,^[99,107] consecutively. Nevertheless, a much better yield by weight can be achieved ($Y_w > 70\%$)^[108] by the electrochemical expansion process.

To enjoy the distinctive properties of graphene, it is vital to produce and maintain graphene as individual sheets. However, graphene sheets tend to agglomerate and even restack to form graphite through van der Waals interactions.^[110] Therefore, the other viable way to produce solution-processable graphene on a large scale is by reducing graphene oxide (GO).^[111–113] GO is commonly used as the starting point for large-scale graphene production as the raw material (graphite) is naturally abundant. It can also easily produce stable aqueous dispersion by simple and cheap solution processes. Although the full reduction of GO to graphene is almost impossible to achieve, the structure and properties of graphene can partially be re-stored by reducing GO to reduced graphene oxide (rGO). Moreover, different properties in rGO can be achieved using different reduction processes, depending on various final applications.^[114] There are various types of chemicals such as (ascorbic acid, sodium hydrosulfite ($\text{Na}_2\text{S}_2\text{O}_4$), hydrazine hydrate ($\text{H}_2\text{NNH}_2 \cdot \text{H}_2\text{O}$), hydriodic acid with acetic acid (HI–AcOH), thermal and electro chemical reduction processes that can be used to achieve different properties in rGO depending on their final applications. Thermal reduction requires critical equipment and the environment to maintain high temperatures, whereas chemical reduction is a cheaper and easily available option that requires room temperature or a moderate level of heating.^[114]

3.2. Carbon Nanotubes

CNT are 1D needle-shaped (whiskers) allotropes of carbon with a high aspect ratio that demonstrates excellent mechanical properties due to their low density of defects. They have also been recognized as the stiffest and strongest among all existing

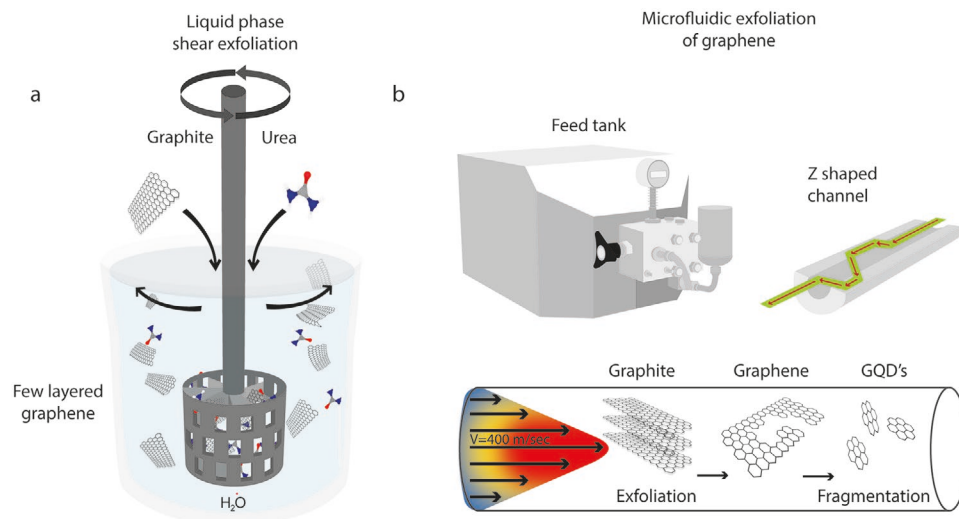


Figure 5. a) Liquid-phase exfoliation of graphite via shear mixing. Reproduced under the terms of the CC-BY license.^[109] Copyright 2020, The Authors, published by MDPI, b) schematic diagram of a typical microfluidizer. The graphite aqueous suspension is powered using a 30 kpsi pump from the feed tank through micron-sized channels. Schematics of Z-shaped channels with diameters ranging from $400 \mu\text{m}$ down to $87 \mu\text{m}$ and a typical flow profile within the channel with a maximal flow speed of 400 m s^{-1} . The graphite flakes are exfoliated into graphene sheets and further fragmented into nanosized graphene quantum dots (GQDs). Reproduced with permission.^[98] Copyright 2016, American Chemical Society.

whiskers, perhaps due to the intrinsic strength of the carbon-carbon sp^2 bond.^[115] These cylindrical large molecules of CNT are made by the hexagonal arrangement of hybridized carbon atoms which are nanometres in diameter and several millimeters in length.^[116] However, due to this small scale, the outstanding properties of CNT can only be exploited if they are homogeneously embedded into various polymers like light-weight matrices. At the same time, it is extremely challenging to disperse and align CNT in a polymer matrix due to van der Waals interactions. Therefore, the production of high-quality CNT reinforced composite heavily depends on the efficient dispersion of CNT into a polymer matrix and the alignment and control of CNT into the matrix.^[117]

Although nanotubes possess a very simple chemical composition and atomic bonding configuration, these are highly diverse and rich in terms of their structures and structure-property relations. Carbon-based single-walled nanotubes (SWNT) are constructed by rolling a sheet of graphene into a cylinder shape along an (m,n) lattice vector, as shown in **Figure 6a**. The (m,n) indices are major parameters of a nanotube that define

the diameter and chirality (the chiral angle between hexagons and the tube axis). SWNT with a nearly similar diameter (1.5 nm) but with different chirality may be either metallic or semiconducting and present band gap as high as ≈ 0.5 eV or as small as ≈ 10 meV.^[118] For same-chirality semiconducting nanotubes, the band gap is inversely proportional to the diameter. Thus, there are endless options in the type of carbon nanotube displaying distinct physical properties.^[119]

While immense possibilities of nanotube structure offer a great range of properties, the major challenge remains in controlling nanotube chirality and diameter. Therefore, delicate control of atomic arrangement along the tube is required to achieve a predictable definite property of the nanotube. Arc-discharge, CVD, and laser ablation are the most commonly used methods for synthesizing carbon nanotubes.^[120]

Arc-discharge and laser ablation are well-established methods for producing high-quality and almost perfect nanotube structures, although these methods produce a large amount of by-products (Figure 6b,c). Such methods require solid-state carbon as precursors for nanotube growth and as

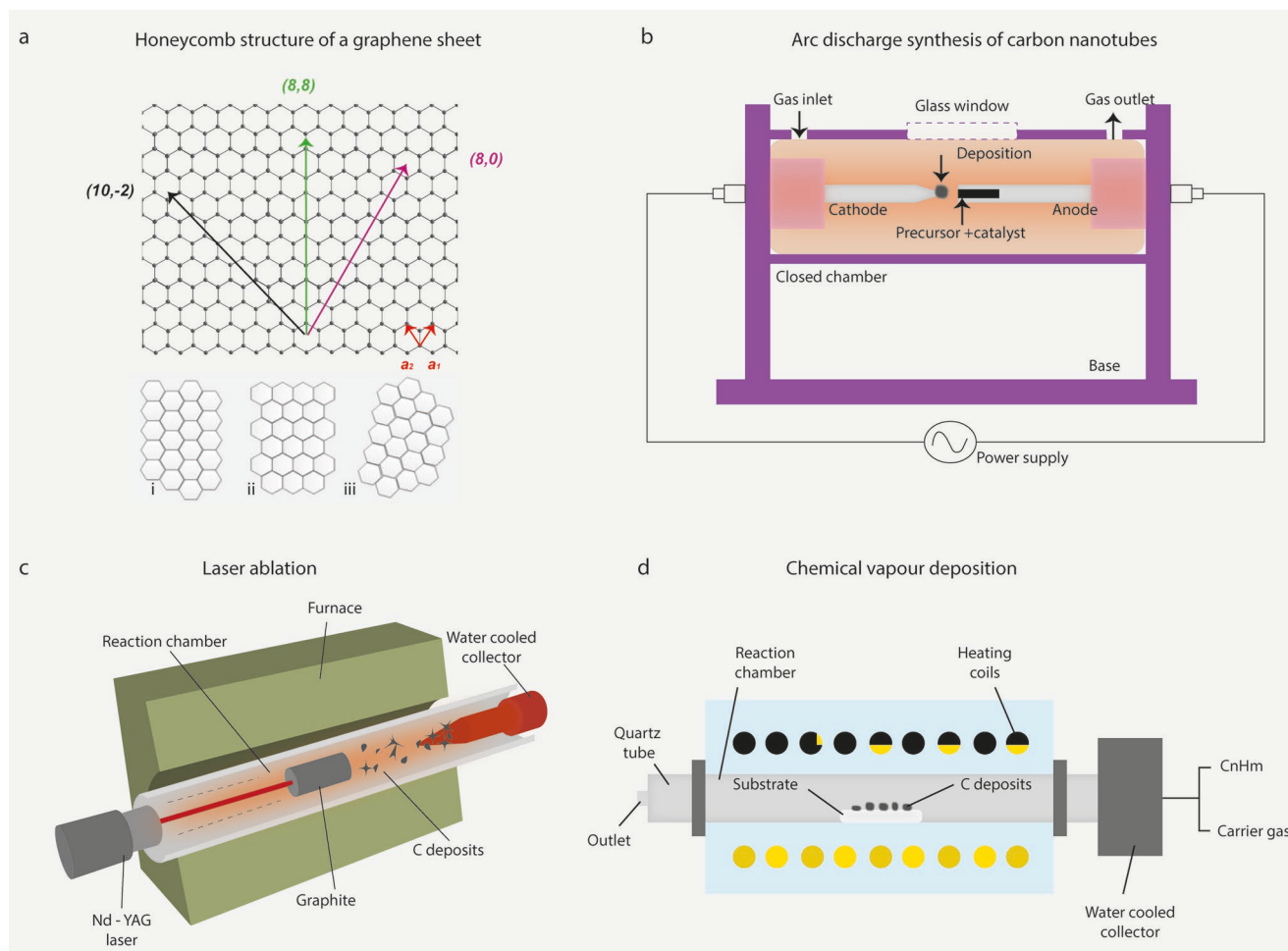


Figure 6. a) Schematic honeycomb structure of a graphene sheet. Reproduced with permission^[119] Copyright 2002, American Chemical Society. Single-walled carbon nanotubes can be formed by folding the sheet along lattice vectors. The two basis vectors a_1 and a_2 are shown. Folding of the $(8,8)$, $(8,0)$, and $(10,-2)$ vectors lead to^[119] various configurations of carbon nanotubes i) armchair, ii) zigzag, and iii) chiral.^[121] Schematic representation of methods used for CNT synthesis b) arc discharge, c) chemical vapor deposition, and d) laser ablation. Reproduced under the terms of the CC-BY license.^[121] Copyright 2011, InTech.

high a temperature as thousands of degrees Celsius for carbon vaporization. In contrast, CVD occurs at moderately lower temperatures (500–1000 °C), where hydrocarbon gases are used as sources for carbon atoms and metal catalyst particles as seeds for nanotube growth (Figure 6d).^[120] However, none of these three methods could produce bulk SWNT materials with homogeneous chirality and diameters, although laser ablation and arc-discharge methods have synthesized SWNT with impressively narrow diameter distributions. CVD methods have been improved from synthesis filaments, CF, and multiwalled carbon nanotubes (MWCNT) to the production of SWNT^[120,122–127] with high crystallinity and perfection comparable to those produced by arc-discharge^[128] and laser ablation^[129] methods.

4. Fabrication Techniques

The incorporation of carbon-based nanomaterials into FRP composites is a challenging task.^[34] Graphene and CNT-based FRP composites have been prepared by incorporating such nanomaterials with reinforcement materials, mixing them into a polymer matrix, or combining both methods.^[51,130–132] In reinforcement modifications, nanomaterials are applied on the fiber surface,^[133] whereas for matrix modification, such materials are dispersed into a polymer matrix before composite fabrications.^[134] In both cases, it is important to form a percolating network of CNT or graphene nanomaterials into the composites to achieve the electrical, thermal, and other multifunctional properties of the composites.^[135] Furthermore, in polymer matrices, GO flakes act as cross-linkers. Such composite materials have adjustable elastic properties and stimuli-responsive properties such as switchable optical^[136] and thermal properties.^[137]

4.1. Reinforcement Modifications

4.1.1. Coating

A coating is a process of depositing a layer of materials onto a substrate to enhance the surface properties or incorporate substrate functionalities. Various coating techniques have been used to deposit graphene and CNT-based materials on the fiber or fabric surface, including dip-coating,^[18,138–142] electrophoretic deposition (EPD),^[133,143–145] spray-coating,^[130] CVD,^[146] and spin-coating. Dip coating is the easiest and cheapest method for the deposition of graphene or CNT on different fiber and fabric surfaces.^[147–149] The dispersion of nano-fillers is prepared in an aqueous or non-aqueous media with the help of mechanical stirring and sonication to improve the dispersibility of the nano-fillers.^[150] The concentration of nano-fillers, solvent type, and fiber dipping time are the key parameters to achieving an effective coating on the fiber surface.

Dip Coating Method: Many researchers^[49,138,154] have used the dip-coating method to manufacture graphene and CNT-based smart FRP composites. Such a method can produce a non-uniform coating on the substrate due to the aggregation of poorly dispersed carbon nanomaterials. In a previous study,^[139] dip-coating was used for coating glass fiber (GF) roving to manufacture graphene-based GF composite as a surface heater for

de-icing application. The coverage of graphene on the GF surface increases with the increase of the number of coating cycles (Figure 7a). The graphene-coated GF roving demonstrated lower electrical resistances and heated up rapidly to a required temperature. The graphene-coated GF rovings were then incorporated into a vacuum-infused GF fabric/epoxy composite, demonstrating the potential use of such composites for de-icing applications. Balaji and Sasikumar^[138] used the dip-coating method for coating GF rovings with rGO to develop a smart composite for in-situ SHM systems. The rGO coated GF was embedded into the GF reinforced polymer composites to monitor the strain and damage induced in the composites by measuring the fractional change in the piezo resistance of the coated fiber. In other studies,^[17,18,24] GO, rGO, and multi-layer graphene flakes were coated on the alkali-treated jute fibers via a dip-coating method. The study showed that the GO is chemically bonded with the cellulosic structure of jute fiber, and graphene flakes are mechanically interlocked with the rough surface of alkali-treated jute fibers, resulting in a uniform deposition of GO and graphene flakes on the fiber surface. Surface modification of aramid fibers (AF) was performed with GO by the dip-coating method to improve the tensile strength and electrical conductivity.^[155] The aramid fibers were treated by plasma and then dip-coated into GO-polydopamine (PDA) solution and obtained GO-PDA-AF. The GO-PDA-AF were converted to rGO-PDA-AF through the reduction by hydrogen iodide and significant improvement of the tensile strength and electrical conductivity were achieved. In another study,^[156] to investigate the interfacial properties, a multi-scale CF/CNT reinforcement was prepared by a one-step dipping method while the common coupling agent 3-glycidyl ether oxy-propyl trimethoxy silane (KH560) was used as the bridge. It was found that the mass fraction of KH560 is a key factor for CNT absorbing on CF surfaces and CNT were uniformly distributed on the CF surface, which confirmed that KH560 is an effective coupling agent for CF and CNT.

Electrophoretic Deposition: EPD is a method of coating nano-filler particles suspended in a fluid under the influence of an electric field applied between the substrates and the counter electrode. EPD is usually carried out in a two-electrode cell, immersed in a dispersion of charged nano-particles by applying the voltage.^[145] EPD is the most common technique used to deposit the nanomaterial on different substrates. Pristine graphene is inappropriate for such coating, as it cannot be dispersed uniformly in most aqueous solvents due to its hydrophobic nature. GO has an oxygen functional group that is hydrophilic and releases a negative charge in the solution. Therefore, an aqueous suspension of GO is a favorable choice as a starting material for EPD. The coating quality and quantity of the nano-particle on the substrate depends on the concentration of nanoparticles in the suspension,^[157] the stability of the suspension, deposition time,^[158] and the applied voltage^[159,160] in the system. The coating of the CF and GF rovings and woven fabrics was carried out in aqueous and non-aqueous suspension of GO or CNT using the EPD method. The effect of GO coating on the GF surface with different deposition voltages supplied from 2.5 to 10 V cm⁻¹ at a constant deposition time was studied.^[159] The results showed that the uniformity and amount of GO coating on the GF surface increased linearly with the deposition voltage.

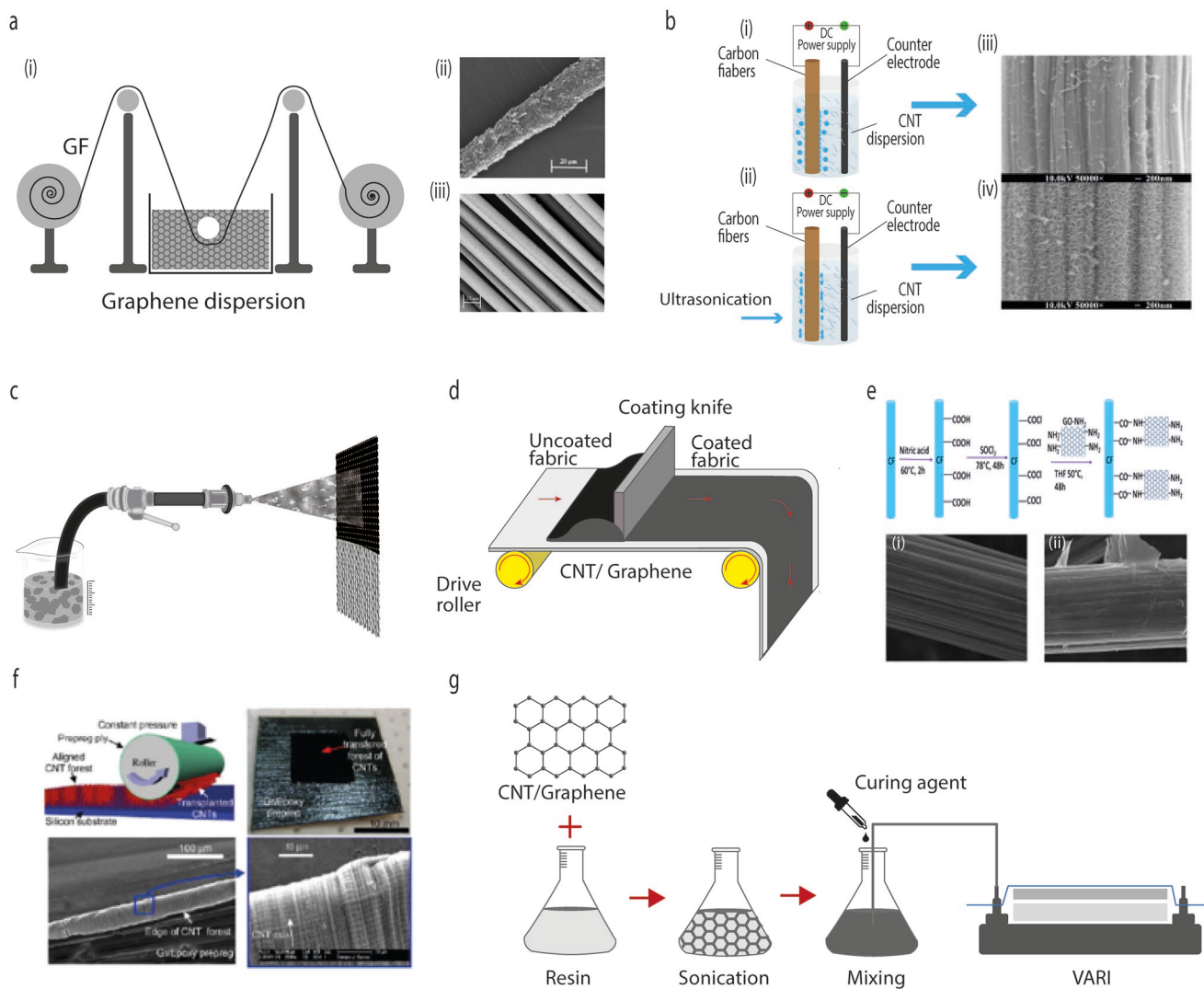


Figure 7. Schematic of different techniques to incorporate nanomaterials in FRP composites. a) i) Dip coating of fiber/fabric into nanomaterial ink, SEM images of ii) graphene-coated glass roving, and iii) untreated glass fiber roving. Reproduced under the terms of the CC-BY license.^[139] Copyright 2018, The Authors, published by Royal Society of Chemistry. b) Schematic of the EPD process of CNT onto carbon fibers i) without ultrasonication, ii) with ultrasonication; SEM images of carbon fiber filaments iii) CNT deposited without ultrasonication and iv) with ultrasonication. Reproduced with permission.^[151] Copyright 2011, Elsevier B.V. c) Schematic of spray coating of nanomaterials on the fabric surface, d) schematic of blade or knife coating of nanomaterials on fabric. e) Schematic of the grafting process and the SEM images of the i) untreated and ii) GO treated CF. Reproduced with permission.^[152] Copyright 2016, Elsevier Ltd. f) Transfer printing process, transplanted CNT forest on the prepreg surface and SEM images of the vertical aligned CNT on prepreg surface. Reproduced with permission.^[153] Copyright 2008, Elsevier Ltd., and g) Schematic of nanomaterials mixed with a thermoset resin and incorporated into composites.

In the EPD process, the bubbles can be formed at working and counter electrodes, affecting the deposition quality and quantity. Sonication during EPD can improve the deposition performance. The effect of ultrasonication during the EPD process on the CNT and GO deposition on the CF surface was investigated.^[151,161] The ultrasonically assisted EPD process increased the thickness and uniformity of CNT and GO coatings on the CF surface compared to EPD only coating process (Figure 7b). The ultrasonic treatment reduced the effect of water electrolysis which improved the coating quality on the fiber surface.

To improve the conductivity of composite materials, the coated GO is converted to electrically conducting rGO by sub-

sequent treatment. Chen et al.^[144] deposited the GO onto the CF surface through the EPD method. Then GO-coated CF was chemically reduced to rGO-coated CF via a subsequent chemical reduction method. The GO-CF and rGO-CF were used to manufacture the composites for EMI shielding application. GO/CNT hybrid materials were also used to coat the CF fabric via the EPD method. The coated CF fabrics were thermally annealed at 200 °C for 2 h before composites manufacturing to convert GO to electrically conducting rGO.^[133] MWCNT and SWCNT were also uniformly deposited on the surface of CF fabric by the EPD process.^[162] Additionally, a comparative study between EPD and dip-coating methods to deposit the MWCNT on the non-conductive GF surface^[80] reported that the EPD

coating method produces a more homogeneous and continuous nanotube distribution on the GF surface compared to the dip coating. Hence, the EPD method proved to be a more effective technique for depositing MWCNT onto the GF surface.

Spray Coating: Spray coating is another coating technique widely used for the deposition of graphene and other 2D materials on fiber and fabric surfaces.^[130,163,164] A schematic of the spray coating is shown in Figure 7c. Spray coating is an effective way to apply nanomaterials coating to irregularly shaped surfaces to obtain desired properties. The most commonly used apparatus for spray coating is the airbrush gun connected to an air compressor. Zhang et al.^[130] prepared CNT/methanol dispersion and deposited them onto CF prepreps using a spray coating method. After spray coating, the solvent was evaporated via applying heat and obtaining a good control of CNT network on the surface. Composite was then manufactured from CNT coated prepreg via a vacuum bag molding process. Graphene nanoplatelets (GNP)/acetone dispersion, containing a small amount of resin and hardener was spread on the CF fabric. It was found that the GNP was well immobilized on the fabric surface.^[163] In this case, acetone worked as a carrier of GNP and later evaporated, leaving GNP-coated fabrics used for manufacturing the composites with the VARI process. The study suggested that the spray coating technique was an effective approach to depositing GNP on dry carbon fabrics. Graphene and CNT-coated conductive Kevlar fibers were fabricated through layer-by-layer spray coating.^[164] Polyurethane was used as the interlayer between the Kevlar fiber and nanomaterials to bind nanomaterials coating into the Kevlar fiber surface. Nanomaterials grafting with co-polymer via free radical polymerization is also used for the spray coating process.^[165] MWCNT and vapor-grown carbon nanofibers (VGCNF) were grafted with poly(styrene-co-maleic anhydride) (SMA) and poly(glycidyl methacrylate) (PGMA) via free radical polymerization and suspended in ethanol. Pristine VGCNF and MWCNT were also suspended in ethanol. Pristine VGCNF and MWCNT suspension agglomerates and precipitations after the ultrasonication were stopped, but VGCNF-g-SMA and MWNT-g-SMA suspension remained stable in ethanol for a long time. The grafted nanotubes and nanofibers were then spray-coated on a CF fabric to manufacture the composites. Natural fiber fabrics were also coated with CNT suspension and the composites were fabricated by VARTM methods.^[166] The stable and uniform dispersion of the CNT in the suspension played a key role in the CNT distribution on the fiber surface. CNT in a mixture of ethanol and water with polyvinyl pyrrolidone (PVP) dispersant provides a stable dispersion and better coating quality.

K Control Coater: The K control coater is another coating system used for surface coatings, as in Figure 7d. to quickly produce a defined uniform coating. The thickness of the coating is controlled by wire wound bars or gap applicators. This process is suitable for bulk production with a thick coating. The K control coater has been used to coat CF fabrics with an aqueous dispersion of MWCNT in an epoxy binder to improve the interlaminar fracture resistance.^[167] The CF fabrics were coated using a meter bar at 6 m min⁻¹ speed, which gives a nominal wet coating thickness of 6 μm. The blade coating technique was also used to apply a uniformly thin film of liquid ink onto moving webs. Tzounis et al.^[168] used the wet-chemical blade

coating deposition process for coating the unidirectional (UD) GF fabric with SWCNT. This process is suitable for large-scale production and the processing costs are very low.

4.1.2. Chemical Grafting

Chemical grafting is another approach to incorporating nanomaterials on the fiber surface. In this method, the nanomaterials are assembled on the fiber surface using a covalent bonding through bridging agents, which introduces functional groups onto the fiber surface. The GO was chemically grafted onto the GF surface by an amidation reaction to improve the interfacial adhesion of GF/epoxy composites.^[169] The GF surface was modified by a silane coupling agent with an amino group and the GO was covalently grafted onto the GF surface by an amidation reaction. FTIR results showed that the GO was covalently immobilized on the GF surface.

The surface modification of aramid fibers was carried out by self-polymerization of poly(dopamine) (PDA) and then GO grafted on the surface of PDA-coated aramid fibers.^[170] The chemical composition and functional groups on untreated and PDA-treated aramid fiber were characterized by X-ray Photoelectron Spectroscopy (XPS). The study suggested that the GO-PDA treatment increased the surface activation of aramid fiber and thus increasing their interfacial adhesion strength.

GO grafting on the surface of CF by using poly(amido amine) (PAMAM) as a bridging agent was investigated by Li et al.^[171] The study indicated that chemical reactions between PAMAM and CF increased amino density on the CF surface. Finally, GO was chemically grafted onto the CF by PAMAM bridging, which changes the surface configuration of the CF. To replace the expensive PAMAM grafting method, another method of grafting for functionalized GO on the CF surface was developed.^[152] In this process, CF fiber was oxidized via nitric acid, followed by acyl chloride treatment. The acyl chloride treated CF was covalently grafted with amino-functionalized GO in the presence of tetrahydrofuran (THF) and formed a new hierarchical structure with increased CF surface roughness (Figure 7e). These GO sheets could stick in the composite interface region, and the functional groups on the GO surface could react with the epoxy resin.

To minimize a change in electronic properties, 2D materials are decorated via different non-covalent techniques, including surface-initiated atom transfer radical polymerization using self-assembled amine-pyrene linkers^[172] or self-initiated photografting and photopolymerization.^[173] Furthermore, functional groups of GO allow chemical and physical binding to polymer matrix and fibers.^[174] The hydrophilicity of GO allows its dispersion in aqueous solutions of water dispersible monomers, polymers, and fibers.

4.1.3. Direct Method

In the direct method, nanomaterials such as CNT, graphene or graphene derivatives are directly synthesized on the fiber surfaces, which then has been used for manufacturing smart composites. Different methods have been used to grow CNT on

the fiber surface, including electric arc-discharge,^[175] laser ablation,^[176] and CVD.^[119,177,178] It was reported that CNT could be grafted directly on the fiber surface.^[179–182] A pre-treatment of fiber was required for the direct growth of CNT on the fiber surface. Zhang et al.^[181] reported that the temperature and feed rate of xylene/ferrocene in the reacting furnace influenced CNT growth mechanism, CNT density, and morphology on the CF surface. Moderate temperature (750 °C) and slower feed rate (5 sccm) were suitable for stable growth and uniform length of CNT on the CF surface. The CVD process was used to deposit CNT on the surface of 2D woven fabrics of SiC to produce 3D fabric for manufacturing multifunctional composites.^[183] The study showed that the CNT was grown on the fabric surface uniformly with ≈60 μm length. The direct method can deposit a higher amount of graphene or CNT on the fiber or fabric surface with controlled alignment and free from agglomeration and filtration-related problems. One of the issues with such a process, which might limit the application, is the possible fiber degradation during processing.^[184–186]

4.1.4. Printing

Printing is another method of applying nanomaterials onto flexible, rigid, and conformable surfaces in definite patterns or designs. Based on the design, the quantity of production, and printed substrates, several printing processes exist such as screen, gravure, flexographic, transfer, and 3D printing. Only a few works have used the printing technique to deposit graphene and CNT on the fiber or fabric surface for manufacturing smart composites. Graphene and CNT dispersions can readily be formulated into functional inks for printing by adding binders, additives, and solvents.^[187] Such functional inks can then be printed on fabric-based reinforcement materials via various printing methods in a random or pre-defined pattern to manufacture smart FRP composites. The graphene or CNT printed preforms can bring functionality to the end product. A conductive path has been produced on the woven fabric surface using graphene ink by the inkjet and screen printing method.^[188,189] Such a technique can be used to prepare graphene-based textile preforms to manufacture smart FRP composites.

Transfer printing which transfers the design from one medium to another enables heterogeneous assembly of different materials into various surfaces arranged in 2D and 3D layouts.^[190] Groo et al.^[191] used the laser-induced graphene to print graphene layers onto polyimide tape using a carbon dioxide infrared laser, which is then integrated on the GF prepreg surface via the transfer printing process. The conductive path created by such techniques was then used for smart composites applications. Additionally, the transfer-printing process was used to transfer aligned CNT to the prepreg, maintaining CNT alignment in the through-thickness direction and manufacturing of composites.^[153] The prepreg is attached to a cylinder rolled across the silicone substrate containing CNT forest and transferred CNT forest on a CF/epoxy prepreg. The SEM image clarifies that CNT forest maintains vertical alignment on the CF prepreg surface after transplantation. The schematic of the transfer printing process, transplanted CNT forest on the prepreg surface, and SEM images of the vertical aligned CNT on the prepreg surface are shown in Figure 7f.

4.2. Matrix Modification

The matrix, a homogeneous and monolithic material, holds reinforcement fibers in its place for FRP composites and plays a significant role in the mechanical properties of the composites.^[192–195] Two major classes of polymers, such as thermoplastic and thermoset, can be used as matrix materials to manufacture FRP composites. Thermoset polymer matrix is a low viscosity reactive liquid, which is uncured at room temperature and suitable for easy impregnation of reinforcement fibers. Composites manufactured with thermoset matrix provide exceptional mechanical properties and a wide range of environmental stability. In contrast, a thermoplastic polymer matrix is a linear chain molecule that is softened by exposure to heat and stiffened by cooling in a temperature range. The advantages of thermoplastic–matrix composites are lower processing time, weldability, higher damage resistance, and recyclability.

The introduction of graphene and CNT into the matrix is one of the modification techniques that have been introduced to increase the toughness, interfacial, mechanical, and multifunctional properties of the composites.^[30,196,197] In this process, the graphene and CNT are mixed with resin and then infused using the existing resin impregnation system (Figure 7g). Therefore, the mechanical and functional properties of FRP composites strongly depend on the dispersion state of graphene and CNT in the polymer matrix. The integration of graphene or CNT and their dispersions into polymer matrices are challenging due to complexities with the aggregation of nanoparticles, viscosity control of dispersion, dispersion flowability through the reinforced materials, and filtration effects during the infusion into the fibers.^[198–201] The leading causes of the poor dispersibility of graphene in the matrices are their large van der Waals forces and strong π – π interactions between the graphene lamellae.^[110,202] Similarly, CNT can easily aggregate due to their larger aspect ratio. The dispersibility of graphenes and CNT can be improved in various ways, such as through physical dispersion methods, and covalent and noncovalent bonding methods.^[203] In the physical dispersion method, a high shear force is applied to break up the aggregation of the graphene and CNT materials for achieving a homogenous dispersion without further material damage. Additionally, a three-roll-mill dispersion, mechanical stirring, and ultrasonic dispersion are used to obtain a homogenous dispersion.^[204–206]

Many researchers have attempted to manufacture smart FRP composites by incorporating graphene or CNT in the matrix.^[30,196,197] They reported that the graphene and CNT content and their dispersibility influenced the functional properties of composites. Double walled CNT (DWCNT) were mixed with epoxy resin, and the CF/epoxy/DWCNT composites laminates were manufactured by vacuum bagging resin infusion process to study the electrical conductivity of composites.^[207] The study showed that DWCNT did not reach inside the CF intra-tow region because DWCNT aggregates are larger than the gaps between CF tows (known as “filtration effect”). However, DWCNT migrated in the through-thickness direction of composites. The overall distribution of the DWCNT inside the composites was uniform. The multiscale composite was manufactured from epoxy resin reinforced with GNP and GF to investigate the electrical conductivity.^[134] Probe sonication and calendaring process were used to disperse the GNP into the epoxy

Table 1. Comparison of different reinforcement and matrix modification techniques.

Techniques	Advantages	Disadvantages
Dip coating	Convenient and facile, low cost, the layer thickness can be easily adjusted, suitable for complex shape, appropriate for use in the lab, suitable for large-scale production	Slow process, subsequent treatment process may be required, inconsistent quality.
EPD coating	Simple process, uniform coating thickness, easy to scale up, can coat the complex substrate, short formation time, thickness of the coating can be tuned.	Difficult to produce crack-free coating, require high sintering temperature, bubble can be formed at working and counter electrodes.
Spray coating	High deposition efficiency, high deposition rate, suitable for thick layer coating	Spraying on complex shapes and the internal surface is difficult
Direct method	Higher deposition amount, possible to control of alignment, no agglomeration, and filtration problem.	Not suitable for mass production, cannot be coated with natural fibers.
Printing	Suitable for random or pre-defined patterns, suitable for thick layer printing.	Fabrication cost is high
Matrix modification	A most convenient way to incorporate the graphene and CNT in the composites using the existing resin impregnation system.	Agglomeration and filtration of the graphene and CNT can happen.

resin. The composite was then manufactured by using a hand lay-up and hot plate pressing method. A microscopic study showed that GNP contents inside the inter-tow space were lower than those observed between fabric layers, confirming filtering phenomena through the laminate thickness.

Surface modified and unmodified CNT were mixed with commercial epoxy resin and infused into CF and GF fabric via the RTM process and laminates performance was investigated.^[198] The variation of the through-thickness electrical conductivity of the CNT-filled CF composite as a function of the distance from the inlet gate was observed. The variation was found to be less for modified CNT-filled composites. These results indicated that the filtration of the CNT occurred in the processing of multiscale CF composite, and it was less in the case of modified CNT filler. The different GO content (0.1–0.7 wt.%) was added through the matrix to the reinforced GF/epoxy composite to study the flexural properties at different temperatures.^[131] The study showed that agglomerates of GO affected the mechanical properties of the composite. The incorporation of 0.5 wt.% GO in the composites exhibited the best results because the higher concentration of nanomaterials increased the viscosity of the matrix leading to filtration of the nanomaterials during infusion through the fiber. To minimize the filtration effect, a simultaneous modification of matrix and fibers has been carried out.^[132] The study showed that MWCNT loading in the epoxy matrix could reach up to 0.075 wt.% to avoid filtration by fabrics. For GNP, GO and rGO, loadings can be tailored according to intended applications. A comparison of different reinforcement and matrix modification techniques is presented in Table 1.

5. Properties of Graphene and CNT Modified Smart FRP Composites

5.1. Electrical Properties

Graphene and CNT can potentially solve one major problem of lower electrical conductivity for smart FRP composites. The composite materials used for conductive applications should have electrical conductivity in the range of 10^{-10} and 10^{-6} S m^{-1} for ESD applications, 10^{-6} and 1 S m^{-1} for moderately

conductive applications, and 1 S m^{-1} or higher for shielding applications.^[208] CF reinforced polymer composites have high in-plane but relatively low through-thickness electrical conductivity and are susceptible to lightning strikes.^[209,210] For some smart composites applications, metallic components are added with FRP composite to make a conductive path; however, it could increase the weight of the component and negatively impact the fuel efficiency.

Electrical properties such as conductivity, EMI shielding, sensing, and Joule heating were among the initial targets for developing smart FRP composites. Graphene and CNT nanomaterials have been added as conductive fillers to non-conductive or less conductive fiber or nonconductive matrix materials to achieve desired electrical properties and save the significant weight of FRP composites. The incorporated highly conductive nanofillers in the composite come in contact with each other and forms a continuous path to enable the traveling of free electrons and conduct the electricity, as shown in Figure 8a. The electrical properties of the FRP smart composite depend on the shape, size, and distribution of graphene and CNT layers in the composite.

The electrical conductivity of the CNT film interleaved CF/epoxy composites with different CNT wt.% were investigated.^[211] The in-plane, out-of-plane thickness, and out-of-plane volume electrical conductivity were improved by 166.7%, 150%, and 60%, respectively, with 1.09 wt.% CNT in the composites compared to CF/epoxy composites (Figure 8b). He et al.^[212] studied the electrical conductivity of CNT-GF/epoxy composite where CNT was homogeneously and perpendicularly grafted on GF using the CVD method to form a core-shell structure. The electrical conductivity of the composites increased with the increase of the weight fraction of the grafted CNT on the GF surface. The in-plane and through-plane electrical conductivity of the composites with 7 wt.% CNT was found to be 100 and 3.5 S m^{-1} , respectively. The electrical conductivity of SWCNT and MWCNT modified CF/epoxy composites were also studied.^[162] The out-of-plane electrical conductivity of the SWCNT/CF/epoxy composite increased 2-fold as compared to CF/epoxy composite. In contrast, the in-plane conductivity remained mostly unaffected by the addition of CNT. Nevertheless, the out-of-plane electrical conductivity of MWCNT/CF/epoxy composites was enhanced by $\approx 30\%$ compared to the reference CF/epoxy composite.

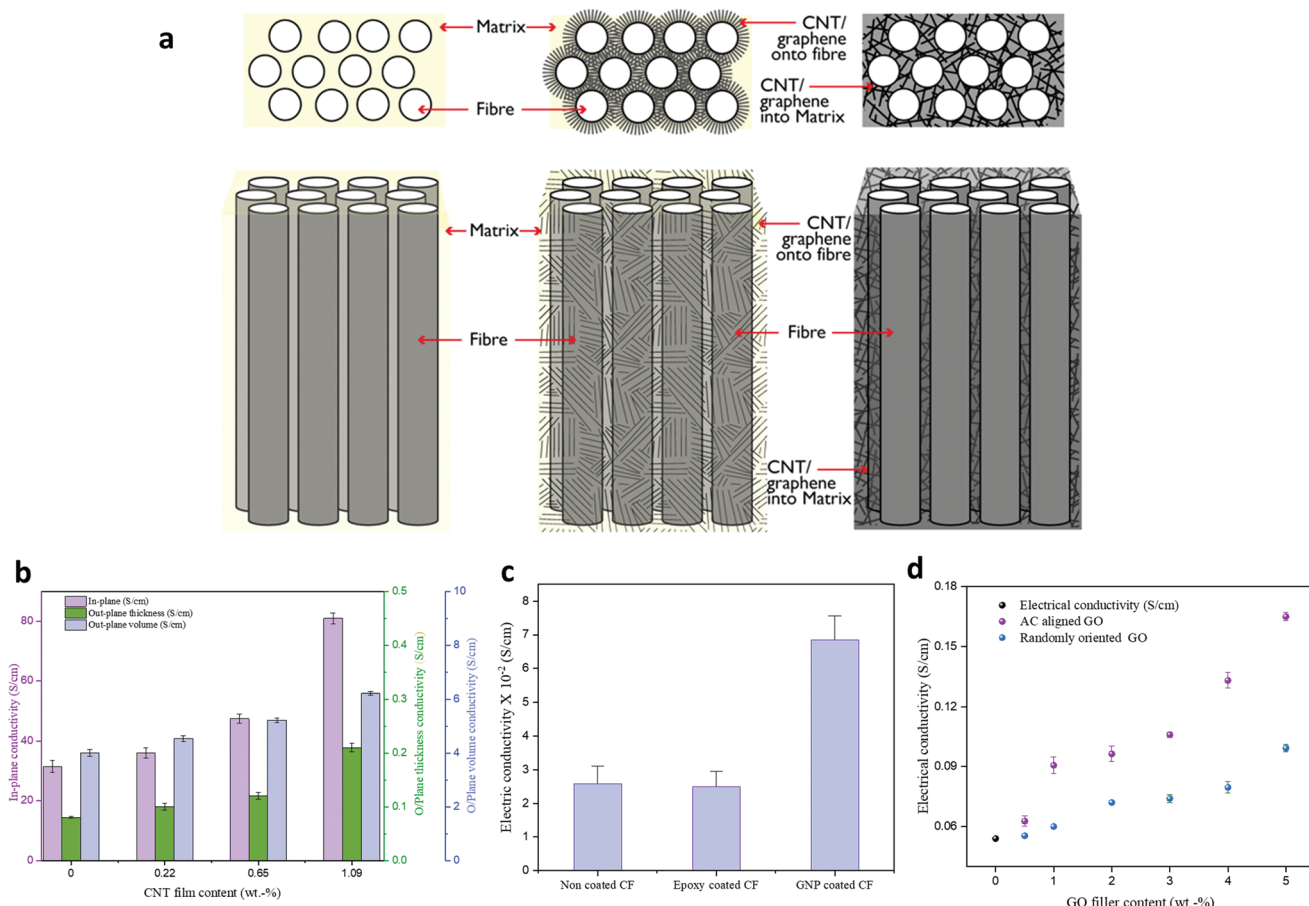


Figure 8. a) Schematic illustration of conventional FRP composites and CNT/graphene-based FRP composites showing the CNT network for the flow of electrons. b) The in-plane, out-of-plane (O/Plane) thickness, and O/Plane volume electrical conductivities of composites with and without CNT film interleaving. Reproduced with permission.^[211] Copyright 2016, Elsevier Ltd. c) electrical conductivity through the thickness direction before and after the adding of GNP in the interphase region. Reproduced with permission.^[51] Copyright 2015, Elsevier Ltd. and d) comparison of the through-thickness electrical conductivity for randomly oriented GO and AC aligned GO-CF/epoxy composites. Reproduced with permission.^[213] Copyright 2020, Society of Plastic Engineers.

The effect of the direction of CNT on the electrical conductivity of composite has also been reported. The unidirectional CF reinforced epoxy composite filled with DWCNT provided increased through-thickness electrical conductivity by one order of magnitude, while the conductivity in the other two directions was not noticeably changed.^[207] In the through-thickness direction, the fibers are connected randomly, depending on the fiber volume fraction of composites. However, with the incorporation of CNT or graphene in the interface, such materials are distributed homogeneously and build up bridges among them, increasing random contacts and resulting in a higher electrical conductivity in through-thickness direction.^[7] In another study on the thermoplastic composite manufactured with SWCNT-polyetheretherketone(PEEK)/CF, it was suggested that conductivity is affected by the direction of the measurement, the degree of fiber impregnation, and the type and concentration of SWCNT.^[214]

The incorporation of GNP in FRP composites strongly influenced the electrical properties of the composites.^[51,134,144] The electrical conductivity has been increased by $\approx 165\%$ in the through-thickness direction of GNP-coated CF/epoxy

composites where GNP created a conductive path between the fibers (Figure 8c).^[51] In another study, the out-of-the-plane electrical conductivity of 5 wt.% GNP modified CF/epoxy composite was increased by almost two orders of magnitude, however, the in-plane electrical conductivity was almost the same as CF/epoxy composite.^[30] The influence of out-of-plane alignment of GO platelets used as matrix filler on the through-thickness of unidirectional CF reinforced composites was also of interest for electrical conductivity.^[213] When the AC field was applied during the composite manufacturing to align the GO perpendicular to the fiber direction, a noticeable improvement in electrical conductivity was observed due to the formation of chain-like paths through the polymer-rich layers facilitating the electrical current and conduction of heat (Figure 8d). The study suggested that less filler content is required in the electric field alignment process in comparison with randomly aligned filler systems to obtain similar improvements.

Graphene materials, such as GO and rGO coated CF/unsaturated polyester (UP) resin composites, have also improved the EMI shielding property.^[144] The GO was coated onto the surface of CF by the EPD process and GO-CF was reduced to rGO-CF

Table 2. Summary of the reported electrical properties of graphene and CNT-based FRP composites.

Composites	Nano filler	Application method	Fabrication method	Electrical Conductivity [% increased or value]	Potential application	Refs.
GNP-CF/epoxy	GNP (1.0%)	Resin mixed	Hand lay-up followed by vacuum bagging and compression molding	+132% ($1.31 \times 10^{-3} \text{ S m}^{-1}$)	Moderately conductive applications	[196]
GO-CF/DVB-PANI	PANI-GO (15%, 60:1)	Resin mixed	Hand lay-up followed hot-press	150% ($6.36 \times 10^{-2} \text{ S m}^{-1}$)	Moderately conductive applications	[50]
GNP-CF/epoxy	GNP (5%)	Resin mixed	VARI	(0.6 S m^{-1})	Moderately conductive applications	[30]
GNP-CF/epoxy	GNP (3%)	Dip coating	Prepreg lay-up and auto-clave method	165% ($7 \times 10^{-2} \text{ S m}^{-1}$)	Moderately conductive applications	[51]
GNP-CF/epoxy	GNP (1%) and SnP (0.05%)	EPD	VARTM	GNP 55% and SnP 70%		[209]
prGO-CF/epoxy	prGO (0.0007%)	EPD	VARTM	In-plane 25% through-thickness 350%		[29]
CNT-SiC/epoxy	CNT	CVD	Hand lay-up	$3.44 \times 10^{-3} \text{ S m}^{-1}$	Moderately conductive applications	[183]
rGO-CF/epoxy	rGO (0.5%)	EPD	Casting molding method	7.20 S m^{-1}	Shielding applications	[215]
CNT-CF/epoxy	CNT (1.09%)	Floating catalyst CVD	Hot-press molding method	In-plane 166.7% (80 S m^{-1}), out-of-plane 150% (0.21 S m^{-1})	Shielding applications	[211]
CNT-UD CF prepreg	CNT (7.99%)	Buckypaper	Vacuum bagging autoclave	In-plane 228% (306 S m^{-1}), out-of-plane 425% (0.21 S m^{-1})	Shielding applications	[216]
GO-CF/epoxy	GO (6.3%)	Epoxy	VARTM	Transverse 25% (70 S m^{-1}), Through-thickness 231% (18 S m^{-1})	Shielding applications	[217]
CNT-CF/epoxy	CNT	PT-CVD	VARTM	Through thickness 450% ($9 \times 10^{-3} \text{ S m}^{-1}$)	Moderately conductive applications	[180]
CNT-GF/epoxy	CNT (7%)	CVD	Hand lay up	In-plane (100 S m^{-1}), through-plane (3.5 S m^{-1})	Shielding applications	[212]
rGO-CF/epoxy	rGO	Resin mixed	RFI	4.4 S m^{-1}	Shielding applications	[81]

by a subsequent chemical reduction process. Compared to CF/UP composite, EMI shielding was improved by 6.8% and 16.3% with a 0.75% mass fraction of GO-CF/UP and rGO-CF/UP composites, respectively. The study suggested that rGO-CF can be a good candidate for use as a lightweight EMI shielding material. The conductive network of the graphene and CNT in the FRP composites has been demonstrated useful for in situ damage monitoring of the composite structures. Baltopoulos et al.^[27] presented an approach for the damage inspection of composite structures incorporating CNT in the GF/epoxy composites through electrical resistance tomography. **Table 2** summarizes reported improvements in the electrical properties of the graphene and CNT-based smart FRP composites.

5.2. Thermal Properties

Thermal properties, such as thermal conductivity, thermal stability, and fire resistance, are also important for smart FRP composites applications.^[218] The most thermally conductive materials are highly crystalline, such as diamond, graphene, and metallic. For a constant thermal conductivity, the material structure needs to be isotropic and homogeneous. The thermal conductivity of bulk polymers used for the matrix is usually very low, in the order of $0.1\text{--}0.5 \text{ W m}^{-1} \text{ K}^{-1}$, which is due to

the complex morphology of polymer chains.^[219] An anisotropic structure of the composites gives poor and uneven heat transport across the reinforced fiber and the polymer matrix. To improve the thermal conductivity of non-conductive materials such as polymer matrix, great attention has been paid to incorporating nanomaterials into the composite structure.

The thermal properties of the conductive nanomaterials in the composite are different from than electrical properties of the nanomaterials in the composites. In the case of thermal conductivity, heat is transported via phonons.^[7] The microscopic voids present in the polymeric structure lead to phonon scattering.^[218] The thermal properties of the materials depend on the vibrational and wave-like aspects of the phonon transfer through a crystalline structure. The more defects are present in the crystalline structure, the lower the intrinsic thermal conductivity of the crystal, as defects lead to phonon scattering and reduce the thermal conductivity. However, long continuous crystalline fibers seem to be an interesting approach to improving thermal conductivity.^[220]

Graphene and CNT have been found to be very successful in converting electric energy to thermal energy in a so-called electrothermal effect (i.e., Joule heating). Much effort has been given to enhancing the thermal properties of the FRP composites by incorporating nanomaterials such as graphene and CNT. Thermal properties of different graphene

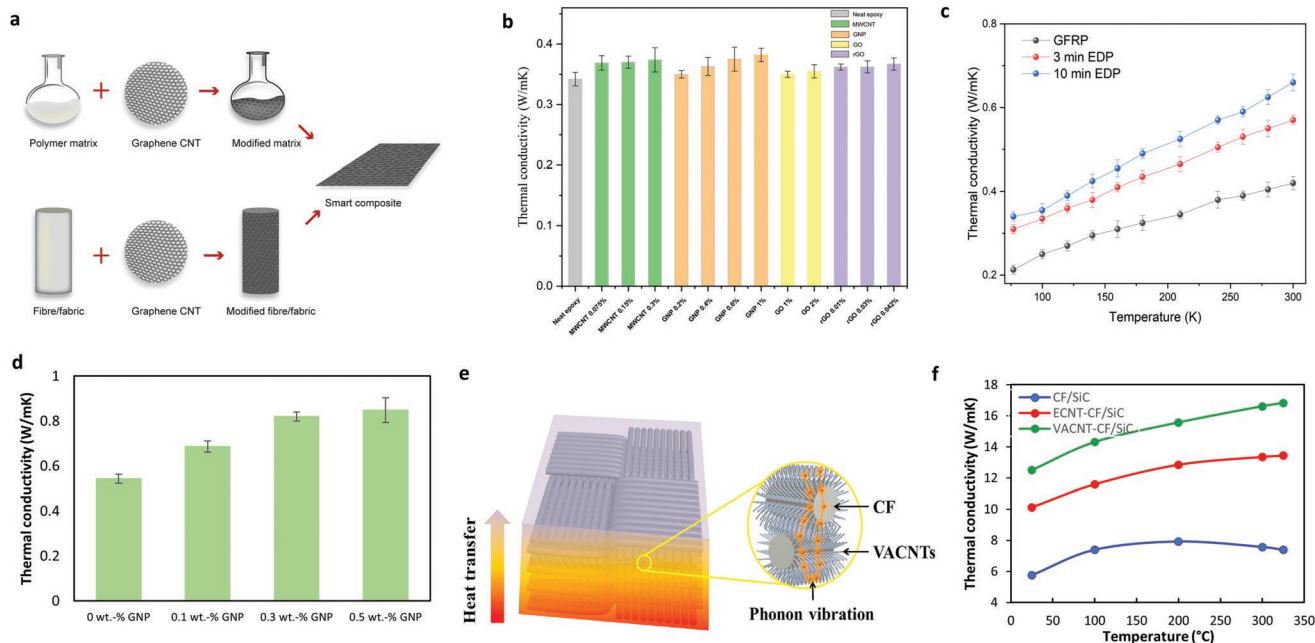


Figure 9. Thermal conductivity of different graphene and CNT-based FRP composites: a) fabrication of graphene and CNT-based GF/epoxy composites and b) their thermal conductivity. Reproduced with permission.^[132] Copyright 2018, Elsevier Ltd. c) thermal conductivity of pure GF and A-MWCNT-GF/epoxy composites as a function of EPD duration time and temperature ranging from 77 K to RT. Reproduced with permission.^[221] Copyright 2014, Elsevier Ltd. d) through-thickness thermal conductivity of the GNP-CF/epoxy composites with different GNP wt.%. Reproduced with permission.^[163] Copyright 2018, Springer Nature. and e) schematic of phonon transport and f) through-thickness thermal conductivity of vertically aligned CNT (VACNT)-CF/SiC composites as a function of temperature. Reproduced with permission.^[76] Copyright 2017, Elsevier Ltd.

and CNT-based nanomaterials, including GNP, GO, rGO, and MWCNT GF/epoxy composites, were investigated.^[132] Additionally, simultaneous modifications of fibers and resins were carried out to manufacture graphene and CNT-based GF/epoxy composites (Figure 9a). It was found that for the same volume fraction of nanomaterials, GNP-based GF/epoxy composites lead to more improvement in thermal conductivity compared to other nanoparticles-based composites (Figure 9b). Furthermore, the thermal conductivity of multiscale MWCNT-woven GF reinforced cyanate ester/epoxy composites was studied as a function of MWCNT deposition time and temperature.^[221] With increasing EPD duration time, thermal conductivities of

nanocomposites are improved for a wide temperature range (from room temperature to 77 K). The thermal conductivity was improved by $\approx 55.4\%$ for MWCNT-GF cyanate/epoxy composites, prepared with an EPD process for 10 min at RT compared to the pure GF cyanate ester/epoxy (Figure 9c). The MWCNT were dispersed with low viscosity polyester/vinyl ester resin and manufactured into the GF composites using the resin transfer molding method.^[222] The incorporation of 3 wt.% CNT in the composites increased the thermal conductivity by $\approx 150\%$. The through-plane thermal conductivity of GNP-CF/epoxy composites laminates increased with the increase of GNP contents due to the formation of the thermally conductive path adjacent

Table 3. Summary of the reported thermal properties of graphene and CNT-based FRP composites.

Composites	Nano filler	Application method	Fabrication method	Thermal Conductivity [% increased and value]	Refs.
CNT-GF/epoxy	CNT (3.88%)	Flame synthesis method	Hand lay-up and hot-press	42.8% (0.544 W m ⁻¹ K ⁻¹)	[227]
CNT-GF/cyanate ester/epoxy	MWCNT (3.74)	EPD	VARTM	55.4% (0.658 W m ⁻¹ K ⁻¹)	[221]
CNT-GF/PEEK	SWCNT (1.0%)	Mixed with thermoplastic resin	Hot press	53% (0.337 W m ⁻¹ K ⁻¹)	[223]
CNT-GF/PA6	CNT (4.0%)	CNT/PA6 film	Hot press	42% (0.058 W m ⁻¹ K ⁻¹)	[224]
GNP-CF/epoxy	GNP (0.5%)	Spray coating	VARI	55.6% (0.84 W m ⁻¹ K ⁻¹)	[163]
GNP -GF/epoxy	GNP (4.0%)	Resin mixed	VARTM	80% (0.342 W m ⁻¹ K ⁻¹)	[197]
GO-GF/epoxy	GO (4.0%)			89% (0.359 W m ⁻¹ K ⁻¹)	
GNP -CF/epoxy				45% (0.406 W m ⁻¹ K ⁻¹)	
GO- CF/epoxy				52% (0.426 W m ⁻¹ K ⁻¹)	
GNP-CF/epoxy	GNP (1.0%)	Resin Mixed	Wet lay-up	9% (0.42 W m ⁻¹ K ⁻¹)	[209]
GNP-CF/epoxy	GNP (1.0%)	Resin Mixed	Hand lay-up and compression molding	6% (0.72 W m ⁻¹ K ⁻¹)	[196]

to fabric plies.^[163] The thermal conductivity was enhanced by $\approx 55.6\%$ with 0.5 wt.% GNP compared to the control CF/epoxy composite (Figure 9d). A scalable process for manufacturing graphene-based surface heating composite for de-icing applications has also been reported.^[139] The composites manufactured from graphene-coated GF rovings into a vacuum-infused epoxy/GF demonstrated potential de-icing applications.

The effects of the pristine graphene and GO inclusions on the thermal properties of the GF/epoxy and CF/epoxy composites were investigated by Zhang et al.^[197] Different wt.% (0.5–4%) of pristine graphene and GO nanoflakes were mixed with epoxy resin. Then CF and GF reinforced composites were manufactured by a VARTM process. The maximum improvement of the thermal conductivity of the composites was achieved when ≈ 4 wt.% nanoinclusion was introduced to the resin. The improvement of thermal conductivity was more distinct for GF composites than CF composites. The result suggested that the GO performs better than pristine graphene in both CF and GF epoxy composites, which may be due to a stronger interfacial bonding between fiber and resin as created by GO, which allows more efficient heat flux and phonon transfer between the two different phases.

The effect of CNT arrangement on through-thickness thermal conductivity in the CF/SiC composites was investigated.^[76] CF fabrics were modified with CNT in two ways – vertically aligned carbon nanotubes (VACNT) and entangled carbon nanotubes (ECNT). The VACNT-CF/SiC composite exhibited the highest thermal conductivity compared to those of the ECNT-CF/SiC and the CF/SiC composites as VACNT favors phonon transport in the through-thickness direction of the composites (Figure 9e,f). CNT-based thermoplastic composites also showed excellent thermal conductivity and low flammability compared to the baseline specimen.^[223,224] The thermal conductivity of CNT/Polyamide-6 (PA6) nanocomposites and woven GF reinforced CNT/PA6 laminates were studied at different CNT concentrations.^[224] Compared to the neat PA6 resin, the thermal conductivity of 4 wt.% CNT/PA6 nanocomposites and corresponding CNT-GF/PA6 laminate (4 wt.% CNT in laminate) was increased by $\approx 180\%$ and $\approx 42\%$, respectively. When 2 wt.% CNT was used in the laminates, and the ignition time and the time peak heat release rate of the laminate samples were delayed by $\approx 31\%$ and $\approx 118\%$, respectively. Shin et al.^[225] investigated the thermal properties of CNT-based CF reinforced epoxy composites by different fabrication methods, such as different CNT mat, buckypaper, and CNT growth on

the CF fabric. The laminates with CNT mats, buckypaper, and the hierarchical showed $\approx 175\%$, $\approx 34.5\%$, and $\approx 22.6\%$ increase in the thermal conductivity over the baseline specimen without CNT. Compared to the direct mixing of CNT into the resin, buckypapers are a more efficient way to improve the fire retardancy of CF composites via delaying the flame ignition, lowering the heat release rate, and less smoke release.^[226] The buckypaper worked as an excellent physical barrier, obstructing the flow of heat and oxygen to the inner polymer resin. **Table 3** summarizes the reported thermal properties of graphene and CNT-based FRP composites.

5.3. Tensile Properties

The mechanical properties of the FRP composites strongly depend on both reinforcement and matrix materials. In high-performance fiber (e.g., carbon, glass, Kevlar) reinforced composites, such properties (e.g., tensile strength, stiffness) of composites are mainly dominated by reinforced material. Li et al.^[228] studied the tensile strength of GO coated short CF reinforced polyethersulfone composite and reported $\approx 12.1\%$ improvement with 0.5 wt.% GO content. The effect of resin/ GNP mixing sonication time on the tensile properties of GNP-GF/epoxy composites was studied. The researchers found that tensile strength increases with the increase of sonication time.^[229] The sonication process changes the morphology of the GNP, which forms progressively more wrinkled with the increase of sonication time. The wrinkled GNP surface can increase the interfacial strength of GNP/polymer matrix due to an additional mechanical interaction, which enhances the ultimate tensile strength of the composite.

CNT was deposited over GF by employing the dip-coating method using Nafion as a binding agent, and the tensile strength and elastic modulus of CNT-coated GF were studied.^[235] At the optimal coating conditions of 1 mg mL^{-1} CNT and 60 min soaking time, the elastic modulus of CNT-coated GF was almost unchanged while tensile strength was increased up to 38%. Another study stated that the tensile strength of the CNT-modified GF epoxy composites depends on the CNT incorporation methods into the composites.^[186] Two incorporation methods were investigated: direct growth of CNT onto GF and dispersion of CNT in the epoxy matrix. The tensile strength of the direct growth CNT-GF epoxy composites decreased by 42%. Still, CNT integration with epoxy matrix enhanced the tensile

Table 4. Tensile properties of the graphene and CNT-based fiber reinforced composites.

Composites	Nano filler	Application method	Fabrication method	Tensile properties [% increases or decrease]	Refs.
rGO-Jute/epoxy	rGO [0.5%]	Dip coating	VARI	183%	[24]
BP/UD-CF	Buckypaper [4.95%]	Buckypaper/ CF prepreg	Autoclave	-4%	[216]
CNT-CF/epoxy	CNT	Resin mixed Dip coating single tow	Single tow composite	69%	[230]
CNT-Ramie/epoxy	CNT [0.7%]	Dip coating	VARI	34%	[231]
GNP-Flax/epoxy	GNP [0.1%]	Resin mixed	VARI	61%	[232]
CNT-CF/epoxy	CNT	EPD	Dipped into matrix	9.86%	[233]
MWCNT-Flax/epoxy	MWCNT [1.0%]	Resin mixed	Hand lay-up	48.7%	[234]

strength by 17%, perhaps due to a higher temperature ($\approx 650^\circ\text{C}$) used during the CNT growth process for the latter.

Natural fiber reinforced composites possess comparatively lower mechanical properties than synthetic fiber reinforced composites, limiting their structural applications. However, recent studies have highlighted that the tensile properties of natural fiber composites can be improved significantly by introducing a small amount of CNT or graphene.^[17,24,231,236] A recent study^[18] reported that nanoengineered graphene-based natural jute fiber epoxy composites enhanced the tensile strength and young's modulus by $\approx 110\%$ and $\approx 324\%$, respectively, compared to jute/epoxy composites. The study also showed that the specific Young's modulus of the composites was $\approx 23\text{ GPa g}^{-1}\text{ cm}^{-3}$, which is higher than that of flax fibers, S-glass, and E-glass fiber composites. Additionally, mechanical properties of rGO-based natural jute fibers/epoxy UD composites were investigated.^[24] The Young's modulus and tensile strength of the rGO-based jute FRP composites increased with the increase of rGO concentrations. The maximum improvement was achieved with 0.5% rGO coated jute/epoxy composites. The rGO coating resulted in $\approx 450\%$ and $\approx 183\%$ improvement in Young's modulus and the tensile strength of the composites. Such remarkable improvements in the mechanical properties of the composites were attained by a combination of physical and chemical treatment together with graphene materials coating of the reinforced materials. Another study

reported that incorporating a small amount (0.1 wt.%) of graphene in the polymer resin of flax fiber reinforced composite increased the tensile strength by 61%.^[232] The effect of the MWCNT as a second reinforcement on the mechanical and thermal properties of polypropylene (PP) biocomposites reinforced with chopped kenaf fiber was also investigated.^[237] The study showed that higher contents of MWCNT (1.5–2 wt.%) were agglomerated, and reduced the tensile properties of the composites. **Table 4** summarizes the reported tensile properties improvement of graphene and CNT-based FRP composites.

5.4. Interfacial and Interlaminar Shear Strength

In FRP composites, the fiber matrix interface plays a crucial role in obtaining desired mechanical properties as the stress is transferred between fiber and matrix through their interface. The incorporation of a small amount of nanofiller such as CNT^[150,162,185] and graphene^[24,49,238] in the FRP composites could significantly improve interface-dominated properties such as interfacial shear strength (IFSS) and interlaminar shear strength (ILSS). Nanofiller improves the fiber/matrix bonding, which plays a vital role in efficient stress transfer, reduces the local stress concentration around the fiber-matrix interlayer, and improves the interfacial properties. Ma et al.^[239] chemically modified the GO nanosheets with cyanuric chloride (TCT) and

Table 5. Interfacial properties of the graphene and CNT-based fiber reinforced composites.

Composites	Nano filler	Application method	Fabrication method	IFSS or ILSS [% increases]	Refs.
GNP-CF/epoxy	GNP [7.9%]	Resin mixed Dip coating single tow		IFSS 34%	[243]
GO-GF/epoxy and rGO-GF/epoxy	GO and rGO	EPD	Hand lay-up method	IFSS 217% for GO 70% for rGO ILSS 15% for GO 9% for rGO	[244]
GNP-CF/epoxy	GNP	Sized (resin) mixed spray coating	VARI	ILSS 24.5%	[163]
GO-CF/epoxy	GO [0.5 mg ml ⁻¹]	EPD	Hand lay-up molding method	ILSS 24.5%	[145]
GO-CF/epoxy	GO	EPD	VARTM	ILSS 56.1%	[245]
MWCNT-Ramie/epoxy	MWCNT [0.6%]	Resin mixed	Hand lay-up and hot press	ILSS + 38%	[52]
GNP-CF/epoxy	GNP 5%	Resin mixed	VARI	ILSS 18%	[30]
GO-GF/epoxy	GO	Chemical grafting		ILSS 41%	[169]
CNT-Flax/epoxy	CNT [1%]	Soaking or spray coating	VARTM	ILSS 20% IFSS 26%	[246]
CNT-GF/Nafion	CNT [1%]	Dip coating	Single fiber	IFSS 116%	[235]
GNP-CF/epoxy	GNP	Solution coating	Prepreg lay-up method	ILSS 19%	[51]
GO-CF/epoxy	GO	Chemical grafting	compression molding method	ILSS 53%	[247]
GO-Aramid/PDA	GO	Chemical grafting	–	IFSS 210%	[170]
prGO-CF/epoxy	prGO [0.0007%]	EPD	VARTM	ILSS 14%	[29]
CNT-SiC/epoxy	CNT	CVD	Hand lay-up	ILSS 54%	[183]
CNT-Ramie/epoxy	CNT	Spray coating	VARTM	IFSS 25.7%	[166]
CNT-CF/epoxy	CNT	EPD	–	IFSS 68.8%	[151]
GO-GF/epoxy	GO	EPD	–	IFSS 219%	[159]

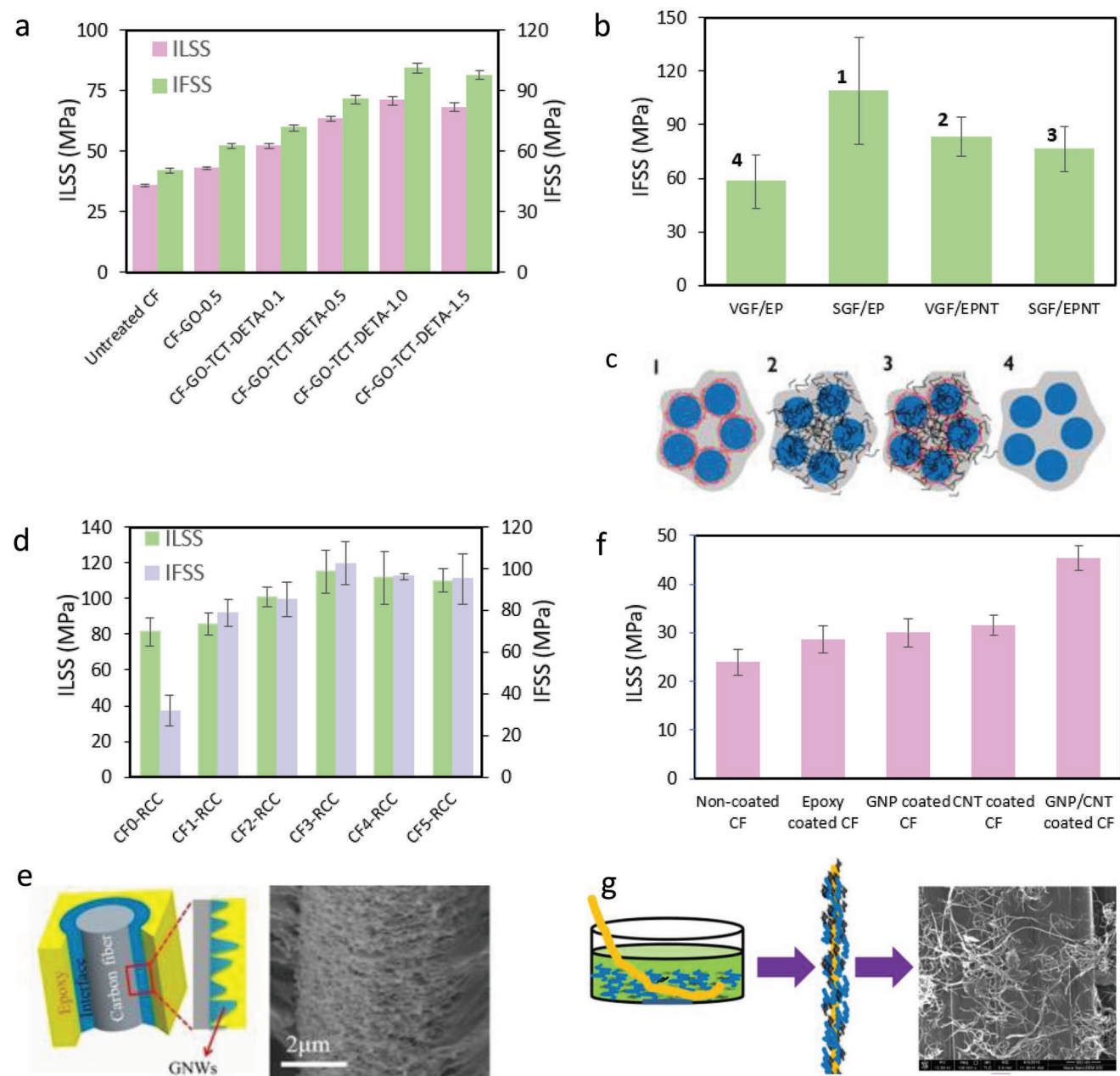


Figure 10. a) IFSS and ILSS of chemically modified GO-CF/epoxy composite. Reproduced with permission.^[239] Copyright 2019, Elsevier Ltd. b) The effect of CNT on the IFSS of GF/epoxy composites and c) schematics of the different material structures, 1). CNT size GF and epoxy, 2). virgin GF and CNT in epoxy, 3). CNT size GF and CNT in epoxy and 4). virgin GF and epoxy. Reproduced with permission.^[56] Copyright 2010, Elsevier Ltd. d) IFSS and ILSS of graphene-modified CF/epoxy composites at different nanowall sizes and e) schematic of composite and SEM image of the fracture surface. Reproduced under terms of the CC-BY license.^[240] Copyright 2020, The Authors, published by MDPI, and f) ILSS of GNP, CNT, and CNT/GNP hybrid coated CF/epoxy composites and g) schematic and SEM image of GNP/CNT hybrid coated CF. Reproduced under the terms of the CC-BY license.^[241] Copyright 2020, The Authors, published by MDPI.

diethylenetriamine (DETA), and deposited them on the CF surface through a sizing agent to study the effect of GO modification on the interfacial adhesion strength of the composites. The best result was obtained by incorporating 1 wt.% GO-TCT-DETA sheets, which improved IFSS and ILSS, by $\approx 104.2\%$ and $\approx 100.2\%$, respectively (Figure 10a). To study fiber matrix interfacial properties of CNT-based GF/epoxy macro-composites,

CNT was introduced to the composites at three different stages: the fiber sizing, in the matrix, and the fiber sizing and matrix simultaneously.^[56] The results indicated that IFSS in all three cases was improved, but the maximum ($\approx 90\%$) improvement was achieved for CNT in the fiber sizing method (Figure 10b,c). In another study,^[49] GO sheets were introduced (7.5 parts of GO contents per hundred of sizing resin) onto the surface

of individual CF through GO modified epoxy sizing, which resulted in an improvement of IFSS by $\approx 70.9\%$ and $\approx 36.3\%$ compared to the virgin CF composites and the commercial sizing agent modified CF composites, respectively. ILSS was also improved by 12.7% compared with commercial-sizing-modified CF composites.

The effect of graphene nanowall (GNW) size on the interfacial properties of CF composites was studied.^[240] GNW was grown on the CF surface using a radio frequency plasma-enhanced CVD method, and the size was controlled by changing deposition time. The study indicates that the size of the GNW affects the IFSS and ILSS of the composites and remarkable enhancement of IFSS ($\approx 222.8\%$) and ILSS ($\approx 41.1\%$) was observed with 45 min GNW incorporated CF/epoxy composites (Figure 10d,e). The synergistic effect of GNP/CNT hybrid coating on the ILSS of CF composites was investigated by Qin and co-workers.^[241] The ILSS of GNP, CNT, and GNP/CNT hybrid coated CF/epoxy composites was $\approx 71\%$, $\approx 73\%$, and $\approx 90\%$ higher than that of non-coated CF/epoxy composites (Figure 10f). A schematic and SEM image of GNP/CNT hybrid coated CF is shown in Figure 10g. A comparative study of the interfacial properties of the CNT and GO coated CF/epoxy composites was carried out, which showed that both CNT and GO improved the IFSS and ILSS significantly, with CNT coated CF/epoxy composites compared to GO coated CF/epoxy composites showed the highest improvement.^[31] A new class of CF co-grafted with GO and CNT was prepared to fabricate composites.^[55] The GO and CNT co-grafting of CF composite improved their ILSS and the IFSS by $\approx 48.12\%$ and $\approx 83.39\%$, respectively. The grafting of GO and CNT on the carbon fiber surface could increase their polar functionality, which leads to an increase in the interfacial properties of the composites.

Recently, Zeng et al.^[154] investigated the effect of the tube- and sheet-like nanocarbons modification of GF fabric on the various properties of epoxy-based composites and explored their reinforcement mechanisms at the fiber/matrix interface. Four different nanocarbons such as pristine MWCNT, carboxyl MWCNT, pristine graphene, and GO were used to manufacture nanocarbon-GF/epoxy composites. All nanocarbon GF/epoxy composites exhibited higher ILSS compared to pure GF/epoxy composites. However, composites containing carboxyl MWCNT and GO showed larger ILSS than that composites containing pristine nanocarbon. Compared to pure GF/epoxy composite, the ILSS was improved by $\approx 16.4\%$ for carboxyl MWCNT-GF/epoxy and by $\approx 29.9\%$ for GO-GF/epoxy. The reinforcement effect of GO on the fiber/matrix interface is superior to that of carboxyl MWCNT. A significant improvement in IFSS after coating graphene materials (GNP and GO) onto jute fibers was reported.^[17] The highest improvement (89%) of IFSS was achieved with 1% GO coated jute fiber. On the other hand, a comparative study on enhancements of mechanical properties of polymer composites reinforced by CNT and GNP sheets using molecular dynamics simulations was conducted.^[242] Molecular models of PMMA matrix reinforced by same weight percentage of CNT and GNP sheet as reinforcement was used. A 5% higher surface crack energy is achieved by incorporating GNP sheet as a reinforcement than CNT reinforcement. It was concluded that the GNP reinforcement plays a better role in delaying the crack propagation than CNT.

The ILSS of the untreated, alkali-treated, GO, rGO, and GNP-coated jute fibers were also investigated using a single fiber micro-bond pull-out test.^[17,24] The ILSS of GO (1%), rGO (0.5%), and GNP (10%) coated single jute fiber composites was increased by $\approx 236\%$, $\approx 97\%$, and $\approx 164\%$, respectively, compared to untreated jute fiber epoxy composites. Such a significant improvement of IFSS with GO-coated fiber is associated with the presence of a huge amount of oxygen functional groups such as hydroxyl, epoxide, carbonyl, and carboxyl in GO. Such functional groups interact with the groups of epoxy resin and form a strong mechanical interlocking at the fiber/matrix interface via suitable bonding. Table 5 shows the summary of the reported IFSS and ILSS improvement of graphene and CNT-based FRP composites.

6. Applications of Fiber Reinforced Smart Composites

The applications of smart FRP composites have been increasing progressively in a wide range of areas such as aerospace, automobile, marine, wind turbine blades, civil engineering, sporting goods, medical application, and other industries. Incorporating nanomaterials in FRP composites will extend its application more widely, such as SHM, electric conductor, thermal conductor, energy storage, and anti/de-icing.

6.1. Structural Health Monitoring

SHM system is capable of continuous monitoring, determining, and classifying the damage inside the composites when a structure is exposed to various environmental and operational conditions. A complete SHM system combines a sensing system, advanced signal processing, damage diagnosis algorithm, and data management system. Different sensing components, including optical fibers,^[248] lead zirconate titanate (PZT) wafers,^[249] metal strain gauges, fiber bragg grating (FBG),^[250] and electromagnetic acoustic transducers (EMTA)^[251,252] have been used to build up sensor networks into an engineering structure. Such methods need cable and wires to connect the individual sensor, which imposes an additional load on the host structure.

FRP composites have widely been used in many structural applications. Great efforts have been made to improve the reliability of such materials by integrating an in-situ SHM system. Graphene and CNT have been used in FRP composites to create percolated networks that allow electrons to pass through the composite and provide the possibility of monitoring internal damage in composites using an electrical resistivity method.^[78,253–255] In FRP composites, damage starts through matrix cracking which is electrically insulating. Therefore, it is necessary to incorporate conductive nanofillers into the composites with fully dispersive sensing networks to achieve enhanced sensing efficiency and accuracy. The acousto-ultrasonics-based SHM where graphene nanoparticles are dispersed into a GF/epoxy composite to form a dispersive network sensing system was investigated.^[256] A small area was required for a single detecting element to capture ultrasonic waves

because of the dense graphene network formed inside the composite. The study concluded that the graphene sensor adds very negligible weight to the host structure and can provide rich information on the structural health status until the failure of the host structure.

An in situ SHM system was developed where the rGO coated GF are embedded in the GF/epoxy composite to monitor the strain and damage induced in the composites by measuring the change in the piezoresistance of the rGO coated GF.^[138] The piezoresistance of the rGO-coated fibers varied linearly under low deformation and nonlinearly under high deformation. The nonlinear piezoresistance indicated the initiation and propagation of microcracks in the composite structures. Similarly, Mahmood et al.^[244] studied the piezoresistive response of GO and rGO coated GF/epoxy composites. The electric resistance of rGO-coated GF/epoxy composites changes proportionally to applied strain, confirming the possible use of such composites for SHM applications.

The effect of CNT dispersion in an epoxy matrix on damage sensing properties under quasi-static loading of GF reinforced composite laminates was studied.^[257] Three roll-milling and fiber sizing techniques were used to disperse CNT in epoxy resin. Uniform dispersion of CNT in epoxy was achieved through three roll-mill techniques. However, non-uniform dispersion of CNT in epoxy was obtained for CNT containing fiber sizing agent. During tensile loading resistance, change per unit length was much lower for the non-uniformly dispensed specimen than the uniformly dispersed specimen because of the higher CNT concentration and agglomerated CNT on the fiber surface.

Some attempts were made to fabricate CNT-based lightweight smart natural fiber composites with damage sensing ability.^[258,259] The electrically semiconducting MWCNT-jute fibers/epoxy composites were manufactured in dog bone-shaped silicone molds.^[259] The study showed that the composites have a multi-functional sensing ability to temperature and stress/strain in the surrounding environment. In another study,^[258] flax fibers were spray-coated with CNT, and reinforced with epoxy resin to fabricate smart FRP composites which was used as a quantum resistive sensor for SHM applications.

6.2. De-Icing and Anti-Icing

The accumulation of ice on aircraft wings,^[83] wind turbine blades,^[260] and power transmission lines^[261] can cause degradation of the structures and huge interruption of their performance. For instance, ice accumulation on an aircraft wing or other parts of the plane can cause loss of aircraft control and increased weight. Developing smart materials to resolve such problems is an active area of research. Two common methods, de-icing and anti-icing are used to overcome such problems. An anti-icing system is intended to prevent the accumulation of ice on the surfaces, and the de-icing technique is designed to remove the build-up ice from the surface.^[262] Many de-icing and anti-icing methods have been used to mitigate the icing problem of different structures, such as pneumatic boots,^[189] hot bleed air,^[190] chemical and mechanical methods,^[260,263] ultrasound systems,^[264] microwave heating systems^[265] and electro-thermal systems.^[139,266,267] The electro-thermal system

is the most energy-efficient for anti-icing and de-icing.^[83] However, an electro-thermal system consists of a metallic component and insulator, which increases the weight of the composite structure.^[262]

The uses of FRP composites in aerospace, automobile, and wind turbine industries are increasing due to their lightweight and outstanding mechanical properties. However, FRP composites have poor electrical and thermal conductivity, limiting their application where the structural surface is exposed to freezing weather. Significant efforts have been made to develop a de-icing protection system into the composite material that can remove ice or slow down its formation on the surface. In this system, graphene and CNT-based conductive composite material are used as heating elements to avoid the accumulation of ice layers by using the Joule heating effect. Joule heating is an electro-thermal system resulting from the dissipation of electrical power generated in an electrically conductive material upon the applied voltage.^[268–270] Recent research showed that graphene and CNT-based FRP composite have significant electrical and thermal conductivity, providing the desired temperature for ice protection without compromising the composite mechanical properties.^[139,266,271,273] Schematic illustration of graphene-based GF smart composite for anti-icing and de-icing application is shown in **Figure 11a**.

A scalable manufacturing process for graphene-based GF/epoxy composite for de-icing applications was reported.^[139] Graphene-coated GF rovings were embedded in the middle of the six-layer GF fabric and then reinforced with epoxy resin to fabricate composite by VARI process. The de-icing test of graphene-based GF/epoxy composite was carried out by dipping the composites into ice bucket at a 10 V electric supply. The temperature of ice bucket with the graphene-based composite increased from -0.1 to 27.3 °C within 5 min, and melted the ice completely. The de-icing performance of the composite is shown in **Figure 11b–e**. The study concluded that the composite could be used as a smart de-icing system for aircraft and other industrial applications.

The de-icing performance of CNT-GF/epoxy composites was investigated where CNT was introduced in the composites as a buckypapers or carbon nanotube paper (CNP) form.^[272,273] An experimental study showed that the surface temperature of the CNT-buckypaper-GF/epoxy composite increased gradually with time, which melted 7 mm of the thick layer of ice completely within 1 h at 6 V power supply.^[273] The de-icing performance of the composite is shown in **Figure 11f–i**. The multifunctional composite can potentially be used in different applications such as aeronautics, aerospace, naval and renewable energies due to their excellent conductivity, electric heating performance, and resistance stability. In another study,^[272] CNP was prepared from SWCNT, Triton X-100, and water. The CNP was presoaked with epoxy resin to prepare the prepreg. Composite was then manufactured using CNP, GF, and epoxy using the compression molding method. The de-icing performance of CNP-GF/epoxy composite at different heat fluxes at -22 °C temperature without wind and with 14 m s^{-1} of wind speed was investigated. It was found that the de-icing times under two conditions were <220 s and 450 s, respectively. These studies suggested that CNT-filled GF/epoxy composite could be used as a self-heating material for de-icing.

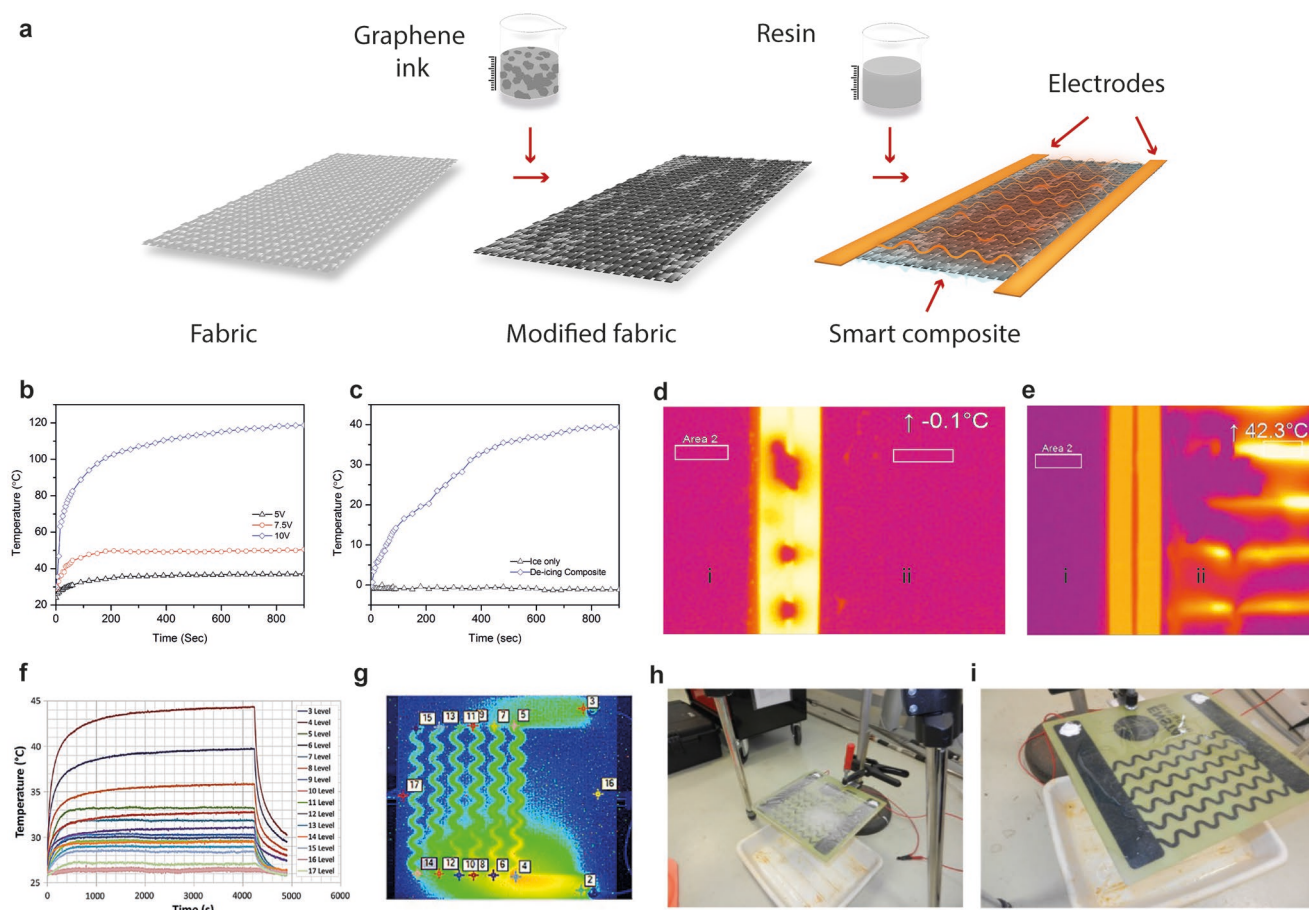


Figure 11. De-icing application of graphene and CNT-based composites: a) Schematic illustration of graphene-based GF smart composite. Deicing test for graphene-based GF composite, b) heating profile at various voltages (5, 7.5, and 10 V), c) the comparative change in temperature of only ice bucket and the ice bucket containing graphene-based de-icing composites, d) thermal images before heating of i) ice bucket and ii) graphene-based de-icing composite dipped into ice showing similar temperature, e) after heating thermal images: i) ice still in the bucket and ii) de-icing composite dipped into ice bucket demonstrates heating of the composites and removal of ice due to Joule heating. Reproduced with permission. Reproduced under the terms of the CC-BY license.^[139] Copyright 2018, The Authors, published by Royal Society of Chemistry. Self-heating and deicing epoxy/GF-based carbon nanotubes buckypaper composites: f) profile of the temperature, g) thermal image, for different points of the composite plate, de-icing test; h) begin of test: panel with ice and i) end of test: panel without ice. Reproduced with permission.^[273] Copyright 2018, Springer Nature.

The arrangement of the CNT network structure in FRP composites influences the electro-thermal properties of the composites.^[266] CNT was embedded in GF composites by two processing routes: the resin impregnation method and buckypapers prepreg method. The de-icing performance of composites was tested at $-20\text{ }^{\circ}\text{C}$ using a 5 V power supply. This study indicated that the resin impregnation pressure method could be an appropriate process for manufacturing the CNT-based self-heating FRP composites for de-icing applications. The graphene and CNT-based FRP smart composites can heat up quickly through the electro-thermal system, indicating these materials could be used for the next-generation anti-icing and de-icing applications.

6.3. Energy Storage in Structural Composites

The incorporation of energy storage devices in FRP composites with a certain level of mechanical performance is a challenging

task. There has been huge interest in making structure and material-based energy storage composites, including batteries,^[274–278] fuel cells,^[279,280] and supercapacitors.^[281–289] A traditional battery depends on electrochemical reactions at the electrodes to deliver energy. In a structure-based battery, traditional electrochemical batteries are embedded into load-bearing FRP composites structures to achieve structural energy storage batteries. In the material-based category, every fabric is engineered to achieve both structure and electrochemical properties.^[290] A schematic illustration of the structural battery and its application is shown in Figure 12a–c.

The structural batteries could potentially be used in electric vehicles, aerospace, marine, and satellites, which can save the weight enormously and enhance the performance of the system.^[291] The previous study showed that when the structural batteries are used in the vehicle structure (Tesla Model S) and (BMW i3), $\approx 20\text{--}30\%$ of weight can be saved without compromising the driving performance. Liu et al.^[292] reported a novel design for a structural composite battery with tunable

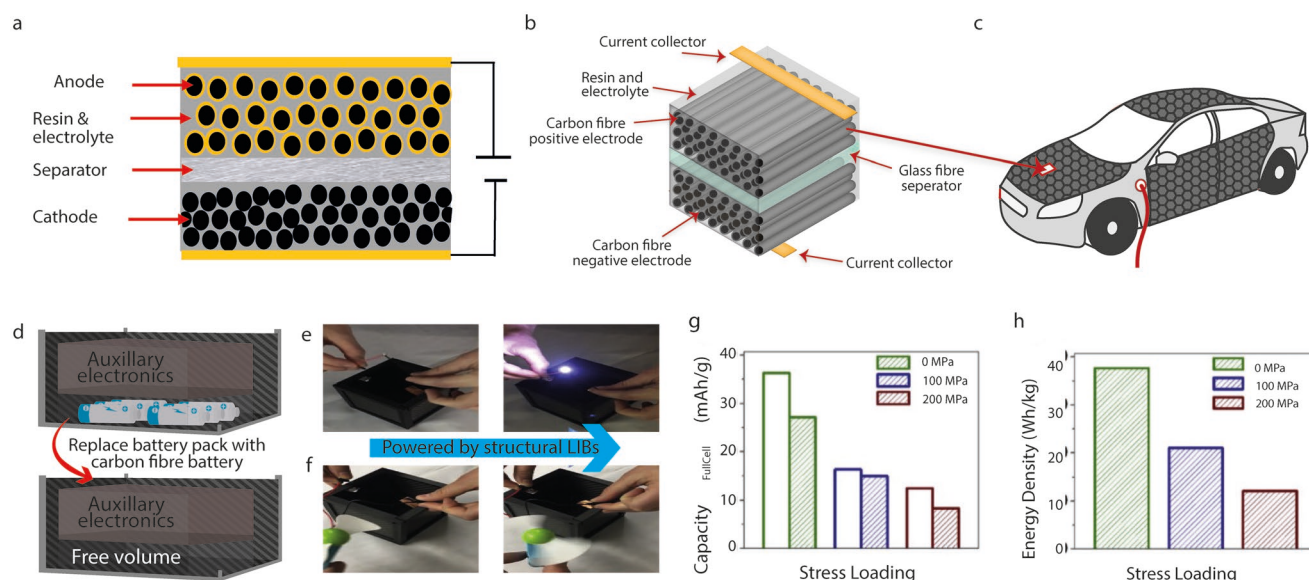


Figure 12. Energy storage application of graphene and CNT-based composites: Schematic of structural battery a) X-sectional image, b) 3D image, and c) its application. CF reinforced structural lithium-ion battery composite replacing interior, external battery pack with structural battery creates free volume within the CubeSat chassis; d) electrochemical performance of structural battery panels in series in a 1U prototype CubeSat frame e) lighting a LED and f) operating a fan, g) mechano-electrochemical performance of CF composite battery charge (outlined bar) and discharge (striped bar) capacity at different stress loadings and h) energy density at different stress loadings. Reproduced with permission.^[293] Copyright 2019, Elsevier B.V.

mechanical properties. A polyvinylidene fluoride (PVDF)-based fiber reinforced solid-state battery was manufactured with different fillers. The cathode of the structural battery was fabricated from carbon fiber, LiCoO_2 , and PVDF as a binder. Anode was manufactured in a similar way to the cathode, with only LiCoO_2 being replaced with graphite. The separator region was reinforced with non-conductive GF. However, the energy density of structural batteries was found to be lower (35 Wh kg^{-1}) than that of conventional lithium batteries. Moyer et al.^[293] fabricated a high-performance structural battery where the active materials for lithium-ion batteries were embedded with CF and epoxy matrix using a traditional layup method. CF as a current collector was used with graphite/CF anodes and LFP/CF cathodes. The composites demonstrated a total energy density of $\approx 35 \text{ Wh kg}^{-1}$ with 213 MPa tensile strength. The study suggested that the lightweight multifunctional structural composite battery could be used for the next generation of power-integrated technologies. The structural battery and its electrochemical and mechano-electrochemical performance are shown in Figure 12d–h. Another research group^[280] developed a structural fuel cell where CF/epoxy composites were used for structural support. The aluminum foam of high porosity is used as the anode and cathode current collector and a carbon cloth as a gas diffusion layer. The power density of the structural fuel cell was found to be 12.5 mW cm^{-2} with a bending stiffness of 2.3 GPa.

Supercapacitors or ultracapacitors are other types of energy storage systems that can store large amounts of electrical energy. Two conducting plates are soaked in an electrolyte and separated by a very thin insulator to store electric energy in a supercapacitor or an electric double-layer capacitor. Graphene and CNT are desirable materials as electrodes for supercapacitor applications due to their higher surface area and better electrical conductivity.^[294–296] A capacitor with both mechanical

load-bearing capability and storing electric energy is called a structural supercapacitor. The European Union-funded project STORAGE demonstrated a structural supercapacitor roof and a trunk lid with supercapacitor laminates made from CF/epoxy insulated by GF that can cut vehicle weight by 60% compared to existing components.^[297] Shirshova et al.^[298] fabricated a structural supercapacitor from two modified CF fabric electrodes separated by GF fabric in CF-GF-CF infused with multifunctional polymeric electrolytes. The addition of nanostructure (carbon aerogel coating) to the carbon fiber surface offers better capacitance to the supercapacitor. This supercapacitor could potentially be used in electric vehicles and the aerospace industry. A structural supercapacitor fabricated from urea-activated graphene nanoflakes (GNF) modified CF fabric electrodes, infused in a mixture of poly(ethylene glycol) diglycidyl ether (PEGDE) polymer matrix and ionic liquid 1-Ethyl-3-methylimidazolium bis(trifluoro methylsulfonyl) imide (EMITFSI) electrolyte offered ≈ 12 times higher energy and power densities compared to control CF specimens.^[299] Such a GNP-based structural supercapacitor can be used in next-generation multifunctional energy storage devices.

6.4. Thermoelectric

The composite materials used for various applications such as aircraft, automotive, and wind turbines are exposed to different temperatures. Graphene and CNT-based polymer nanocomposites were proposed as thermoelectric power generators, as they can generate voltage upon exposure to a temperature gradient.^[300–302] However, such nanocomposites do not fulfill the requirements for thermal stability at high temperatures compared to structural FRP composites. Therefore, the

development of thermoelectric FRP composite is an interesting field of research.^[303] Tzounis et al.^[304] reported that MWCNT-grafted GF/epoxy composite is highly sensitive to UV-light and can be used as an integrated composite sensor and thermal energy harvesting. The thermoelectric properties and potential thermal energy harvesting of CNT-GF/epoxy multiscale and CF/epoxy composites were studied.^[305] Different amounts of CNT (0.5, 1, 3, and 5 wt.%) were mixed with resin in order to manufacture CNT-GF/epoxy multiscale composites. The CNT-GF/epoxy multiscale composites and CF/epoxy composite exhibited *n*-type and *p*-type thermoelectric behavior, respectively. The thermoelectric power of short polyacrylonitrile (PAN)-based CF/polycarbonate composite was investigated and found that the thermoelectric activation energy depends on temperature, frequency, and CF wt.%.^[306] The thermoelectric properties of CNT-filled polymer composite were enhanced by modifying junctions between CNT using poly(3,4-ethylene dioxithiophene) poly(styrene sulfonate).^[307]

6.5. Other Applications

The color change of FRP smart composites is a new type of functionality. The color can be changed under external stimuli such as light, electricity, temperature, pressure, stress, and strain.^[308] Previous studies demonstrated that graphene and CNT reinforced polymer composites can change their color by external stimuli.^[309–311] In recent years, the stimuli-sensitive color changed FRP composite attract interest for structural smart composite applications. Deng et al.^[312] developed graphene-coated GF smart composites that can change color when the composites' structure is deformed. The composite was manufactured from graphene flakes coated single GF and epoxy resin in a dog-bone shape mold and the graphene-coated GF was visible in red color. When the stress was applied, the composite deformed and changed the interference and the color of reflected light, changing the composite color from red to yellow and green. Such smart composite has immense potential for applications in automobiles, aerospace, and other industrial applications as an integrated sensor and SHM. In another study,^[313] the CNT/polydiacetylene nanocomposite fibers rapidly change color from blue to red (visible with the naked eye) in response to electrical current and mechanical stress with very low elongation, which was a reversible process. These electrochromic nanocomposites could be used in many sensing applications. The damage and deformation of self-reporting FRP composites can be visualized by observing the color change of the composites. To achieve such an optical signal dye-filled fluorescent capsules were incorporated into the composites either into a polymer matrix or at the interface between fibers and polymer matrix.^[314]

Elmarakbi^[315] recently developed graphene-based FRP composite material for a prototype car bumper. The bumper is made of CF and graphene reinforced thermoset resin and the small inside ribs are made of GF and graphene reinforced thermoplastic resin. They reported that the graphene-based FRP composite material has 40% higher specific energy absorption than traditional composite materials and can reduce the thickness of the carbon fiber component by 30–40%. The world's first graphene conductive geotextile was launched by Imagine

IM Pty, an Australian-based company in cooperation with Geofabrics Australasia, in 2016.^[316]

7. Perspectives

The global smart FRP composites market is growing progressively due to their higher demand in automotive and transportation, wind energy, aerospace, defense, and sports industries. Specifically, the demand for graphene and CNT-based smart FRP composites is increasing day by day since such materials can add new functionalities to composites by adding a very small amount of weight without sacrificing their mechanical properties. However, the main challenge is how to integrate such nanomaterials into the different phases of composites with existing or modifying the composite fabrication process. In this paper, we overviewed FRP composites based on graphene, CNT, and their derivatives, focusing on the production of these nanomaterials, their incorporation techniques into FRP composites, composite manufacturing processes, and their multifunctional properties and uses. To fully exploit the advantages of the graphene and CNT-based smart FRP composites, the followings need to be addressed.

7.1. Toward High-performance Smart FRP Composites

There is no doubt that smart FRP composites are revolutionizing high-performance composite applications due to their outstanding mechanical and multifunctional properties. The conventional FRP composites will be replaced by smart FRP composites because such materials will greatly influence many multi-disciplinary applications for the composite industry. High-performance fiber and smart materials will be used to manufacture high-performance composites (Figure 13a–c). Graphene and CNT have been considered the most intriguing nanomaterials for developing multifunctional composites. Incorporating such materials into FRP composites is a promising way to achieve multifunctionalities within the composite structure. However, the homogeneous distribution of individual graphene and CNT nanomaterials, their alignment, connectivity, and bonding between matrix and fiber reinforced materials will need to be addressed to attain truly multifunctional composites.

Many laboratory-scale research works have been conducted to deposit the graphene and CNT nanomaterials on the fiber surface. However, there are still numerous challenges to transferring these technologies to industrial-scale production. Many studies reported that the EPD and the dip-coating be scalable industrial processes for depositing the graphene and CNT-based nanomaterials on the fiber surface to fabricate smart composites.^[24,49,80,209] The knife or blade coating process is another feasible industrial-scale production process to modify the reinforced materials with graphene or CNT nanomaterials. In this case, an epoxy-compatible binder can be used to formulate graphene or CNT-based coating inks. Also, the quantity, quality, and agglomeration of graphene and CNT-based nanomaterials in FRP composites will significantly affect the mechanical and functional properties of the composites. Therefore, it is necessary to develop a suitable continuous manufacturing process

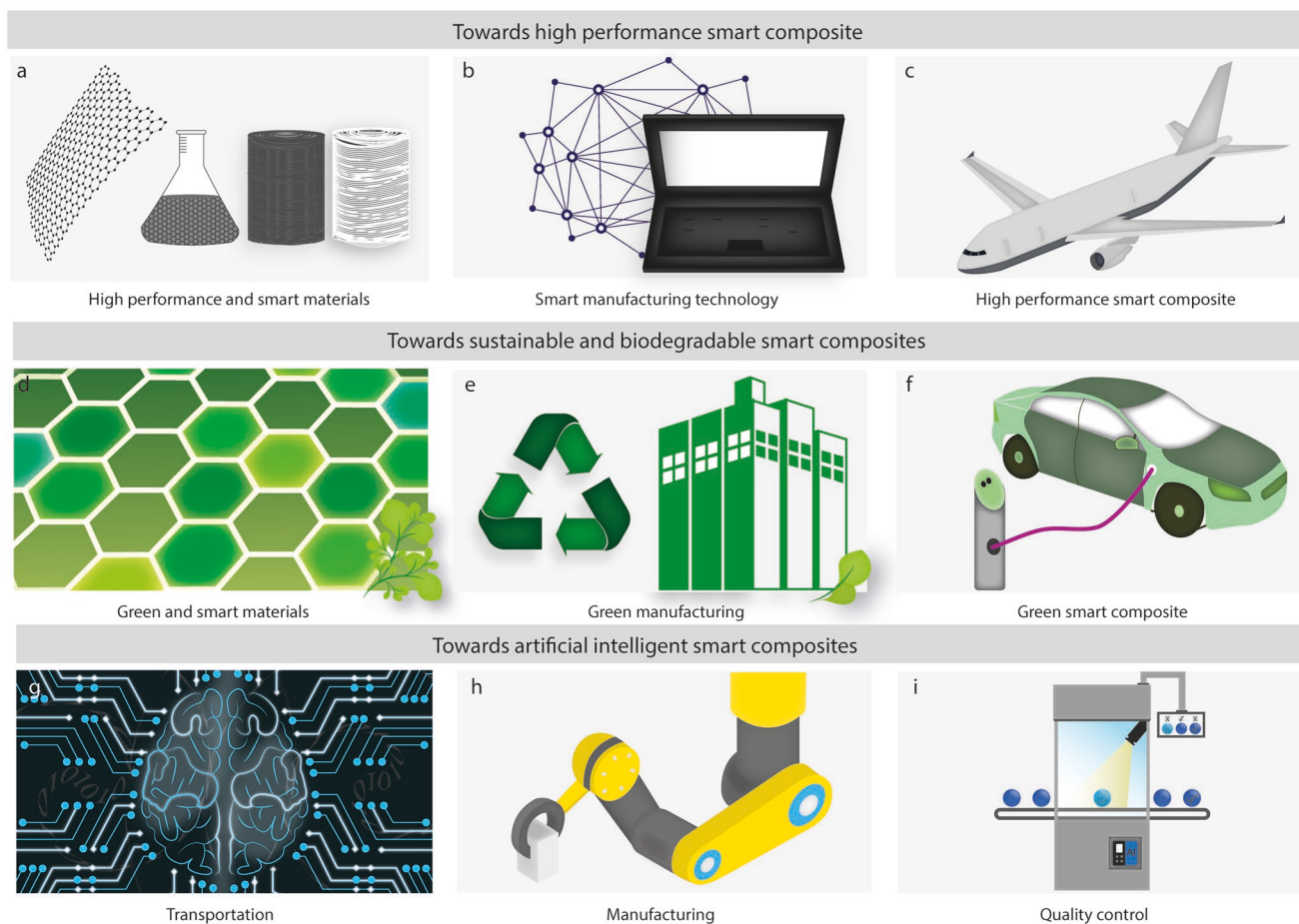


Figure 13. Future research directions and recommendations: a) High-performance fiber and smart materials, b) Smart manufacturing technology used for manufacturing composites, c) Potential applications of high-performance smart composites, d) The use of green and smart materials for manufacturing sustainable and biodegradable smart composites, e) sustainable manufacturing process, f) potential application of sustainable and biodegradable smart composites, g) data preparation of AI-based composite system h) AI-based composite manufacturing system and i) composite inspection and monitoring through AI system.

for nanomaterials coated fiber/fabric preform, where the preparation of agglomeration-free nanomaterials suspension and the appropriate amount of nanomaterials deposition on the fiber surface will be confirmed by online quality control.

Some research reported that mixing graphene and CNT into the resin system and then infusing them using existing resin impregnation systems into the dry fiber arrangement can be scaled up for industrial production. However, the main challenge associated with matrix modification is the aggregation of graphene/CNT.^[198,199] The viscosity of the dispersion increased drastically with the increase of the amount of graphene/CNT. Additionally, filtration effects during the infusion into the fibers can affect the quality of the composites. Different attempts have been made to overcome such difficulties, including the functionalization of graphene/CNT and using an organic solvent with the matrix. Still, more research needs to be carried out to enable a rapid transition for industrial-scale productions.

The aggregation and viscosity are the major concerns for the incorporation of graphene and CNT into the FRP composites. The simultaneous modification of fibers and resin can be a

more viable approach to manufacturing graphene and CNT-based FRP composites.^[132] In this process, half of the nanomaterials will be deposited on the fiber surface to make preform, and the other half will be mixed with matrix before mixed with the nanomaterials coated preform, which will allow a higher amount of nanomaterials into the composites structure. Significant research has been carried out to improve FRP composites' in-plane and out-of-plane properties using graphene and CNT with promising results. There has also been good progress with the improvement of the non-structural functional properties, including the electrical conductivity, thermal conductivity, SHM system, EMI shielding, energy storage, energy harvesting, color change, and self-healing of the graphene CNT-based FRP composites. However, the research and technological developments are still in their infancy for industrial-scale mass production of such composites. Interdisciplinary research and skill development, including materials science, mechanical engineering, polymer chemistry, and chemical engineering, is required to transfer the lab-scale research to industrial-scale mass production of smart FRP composites with multifunctional properties.

7.2. Toward Sustainable and Biodegradable Smart FRP Composites

In recent years, the use of sustainable and biodegradable materials instead of synthetic materials for FRP composites has risen due to growing environmental concerns with synthetic materials.^[317–319] To manufacture entirely green composites for industry, transformative research is required. Materials (reinforcement, matrix, and nanofiller) selection and manufacturing process are vital in producing sustainable and biodegradable smart FRP composites (Figure 13d–f). Natural fibers are sustainable, biodegradable, and available in nature (Figure 13d). For this reason, natural fiber composites have drawn significant research interest over the years due to the advantages of these materials compared to synthetic fiber composites, including low environmental impacts such as less carbon emission, biodegradability, low cost, and density.^[317] However, natural fibre composites suffer from lower mechanical properties such as lower strength, stiffness, poor interfacial properties, and high moisture absorption than synthetic fiber composites. One of the critical challenges in producing sustainable, biodegradable, and lightweight smart materials for structural composites applications is offering specific combinations of stiffness, strength, toughness, and multifunctionalities. A great effort has been made to improve the mechanical and functional properties of the natural fiber composite by incorporating graphene and CNT into the composite's structure.^[18,36,234]

Petro-based non-biodegradable or bio-based non-biodegradable polymer matrices are most commonly used to manufacture FRP composites, which are not 100% green composites. The application of bio-based non-biodegradable composites is increasing in the automotive and other manufacturing industries. Bio-based green polymers (e.g., polylactic acid (PLA)) are considered to be a sustainable alternative as reinforcements or matrices, due to their manufacturing from renewable raw materials and their biodegradation under the specific conditions of industrial composting.^[320–322] The application of such materials is still limited to low-end structural applications due to their poor mechanical properties and cost.^[317,323] Efforts should be given to developing a suitable bio-based biodegradable system to manufacture high-performance and green FRP composite. These composites will help reduce non-degradable plastic waste and improve the overall carbon footprint associated with composites industries.

The inherently sustainable and economical large-scale production process for graphene and CNT nanomaterials is also essential for producing sustainable, biodegradable smart FRP composites (Figure 13e). Due to the increasing exploitation of carbon-based nanomaterials and their subsequent release into the environment, the potentially toxic impact of these materials on human health and the environment should be considered. During the large-scale production of carbon nanomaterials, improper separation, leaching out from developed products, and disposal of consequent waste might cause a significant release and accumulation of carbon nanomaterials in the environment.^[324]

7.3. Toward Artificial Intelligent Smart FRP Composites

The world is moving toward the digital age, requiring smart and environmentally friendly technologies with flexible manufacturing processes. The introduction of new technologies such as robotics, artificial intelligence (AI), and additive manufacturing facilities could be introduced in the raw materials and composite manufacturing process for a cost-effective standard-quality product. AI is a broad discipline that uses powerful algorithms to perform similar tasks to human intelligence (Figure 13g). In the era of the Industry 4.0 revolution, the uses of AI in the field of composite materials are progressively increasing in different fields from research to real-life applications such as design and analysis, material storage, manufacturing, non-destructive testing, and prediction of its remaining useful life.^[325,326] A multifunctional structural system is important for the effective implementation of AI technology in composite materials. A proper sensor system needs to be chosen that can be used in all operational conditions in the composite structure and does not affect the mechanical properties of the composite while integrating them. Graphene and CNT-based FRP composites can provide such facilities. Future development of AI technology should focus on the advanced design and manufacturing process, which can integrate the reinforced matrix and nanofiller to understand the full advantage of the generative design and implement them in the composite structure for the real-time prediction from start to end of life applications (Figure 13h,i).

Acknowledgements

The authors acknowledge UKRI Expanding Excellence in England (E3) funding from Research England and also graphic supports from Laura Wescott and Laura Clarke Oaten. The authors gratefully acknowledge Professor Tawfique Hasan, The University of Cambridge for useful discussion. KSN was supported by the Ministry of Education, Singapore, under its Research Centre of Excellence award to the Institute for Functional Intelligent Materials (I-FIM, project No. EDUNC-33-18-279-V12) and by the Royal Society (UK grant number RSRP/R/190000).

Conflict of Interest

The authors declare no conflict of interest.

Keywords

carbon nanotubes, fiber reinforced composites, graphene, smart composites

Received: May 19, 2022

Revised: June 27, 2022

Published online: August 23, 2022

[1] X. Yu, H. Cheng, M. Zhang, Y. Zhao, L. Qu, G. Shi, *Nat. Rev. Mater.* **2017**, *2*, 17046.

[2] H. Asanuma, *JOM* **2000**, *52*, 21.

- [3] K. Chu, S.-C. Lee, S. Lee, D. Kim, C. Moon, S.-H. Park, *Nanoscale* **2015**, *7*, 471.
- [4] S. Araby, Q. Meng, L. Zhang, I. Zaman, P. Majewski, J. Ma, *Nanotechnology* **2015**, *26*, 112001.
- [5] R. F. Gibson, *Compos. Struct.* **2010**, *92*, 2793.
- [6] N. Yamamoto, R. Guzman de Villoria, B. L. Wardle, *Compos. Sci. Technol.* **2012**, *72*, 2009.
- [7] V. Kostopoulos, A. Masouras, A. Baltopoulos, A. Vavouliotis, G. Sotiriadis, L. Pambaguan, *CEAS Space J.* **2017**, *9*, 35.
- [8] A. Mirabedini, A. Ang, M. Nikzad, B. Fox, K. T. Lau, N. Hameed, *Adv. Sci.* **2020**, *7*, 1903501.
- [9] M. F. De Volder, S. H. Tawfick, R. H. Baughman, A. J. Hart, *Science* **2013**, *339*, 535.
- [10] S. Han, Q. Meng, S. Araby, T. Liu, M. Demiral, *Composites, Part A* **2019**, *120*, 116.
- [11] K. S. Novoselov, A. K. Geim, S. V. Morozov, D. Jiang, Y. Zhang, S. V. Dubonos, I. V. Grigorieva, A. A. Firsov, *Science* **2004**, *306*, 666.
- [12] W. Eom, S. H. Lee, H. Shin, W. Jeong, K. H. Koh, T. H. Han, *ACS Nano* **2021**, *15*, 13055.
- [13] W. Eom, E. Lee, S. H. Lee, T. H. Sung, A. J. Clancy, W. J. Lee, T. H. Han, *Nat. Commun.* **2021**, *12*, 396.
- [14] S. Wan, Y. Chen, S. Fang, S. Wang, Z. Xu, L. Jiang, R. H. Baughman, Q. Cheng, *Nat. Mater.* **2021**, *20*, 624.
- [15] S. Wan, X. Li, Y. Chen, N. Liu, Y. Du, S. Dou, L. Jiang, Q. Cheng, *Science* **2021**, *374*, 96.
- [16] T. Li, A. D. Pickel, Y. Yao, Y. Chen, Y. Zeng, S. D. Lacey, Y. Li, Y. Wang, J. Dai, Y. Wang, *Nat. Energy* **2018**, *3*, 148.
- [17] F. Sarker, N. Karim, S. Afroj, V. Koncherry, K. S. Novoselov, P. Potluri, *ACS Appl. Mater. Interfaces* **2018**, *10*, 34502.
- [18] F. Sarker, P. Potluri, S. Afroj, V. Koncherry, K. S. Novoselov, N. Karim, *ACS Appl. Mater. Interfaces* **2019**, *11*, 21166.
- [19] X. Liang, Y. Gao, J. Duan, Z. Liu, S. Fang, R. H. Baughman, L. Jiang, Q. Cheng, *Carbon* **2019**, *150*, 268.
- [20] Y. Zhang, Y. Li, P. Ming, Q. Zhang, T. Liu, L. Jiang, Q. Cheng, *Adv. Mater.* **2016**, *28*, 2834.
- [21] S. Afroj, L. Britnell, T. Hasan, D. V. Andreeva, K. S. Novoselov, N. Karim, *Adv. Funct. Mater.* **2021**, *31*, 2107407.
- [22] G. Hu, J. Kang, L. W. T. Ng, X. Zhu, R. C. T. Howe, C. G. Jones, M. C. Hersam, T. Hasan, *Chem. Soc. Rev.* **2018**, *47*, 3265.
- [23] H. Park, R. B. Ambade, S. H. Noh, W. Eom, K. H. Koh, S. B. Ambade, W. J. Lee, S. H. Kim, T. H. Han, *ACS Appl. Mater. Interfaces* **2019**, *11*, 9011.
- [24] N. Karim, F. Sarker, S. Afroj, M. Zhang, P. Potluri, K. S. Novoselov, *Adv. Sust. Syst.* **2021**, *5*, 2000228.
- [25] S. Iijima, *Nature* **1991**, *354*, 56.
- [26] O. Breuer, U. Sundararaj, *Polym. Compos.* **2004**, *25*, 630.
- [27] A. Baltopoulos, N. Polydorides, L. Pambaguan, A. Vavouliotis, V. Kostopoulos, *Composites, Part B* **2015**, *76*, 149.
- [28] F. H. Gojny, M. H. G. Wichmann, B. Fiedler, W. Bauhofer, K. Schulte, *Composites, Part A* **2005**, *36*, 1525.
- [29] W. Lee, J. U. Lee, H. J. Cha, J. H. Byun, *RSC Adv.* **2013**, *3*, 25609.
- [30] Y. Li, H. Zhang, Z. Huang, E. Bilotti, T. Peijs, *J. Nanomater.* **2017**, *2017*, 10.
- [31] X. Yao, X. Gao, J. Jiang, C. Xu, C. Deng, J. Wang, *Composites, Part B* **2018**, *132*, 170.
- [32] S. Zhao, Z. Zhao, Z. Yang, L. Ke, S. Kitipornchai, J. Yang, *Eng. Struct.* **2020**, *210*, 110339.
- [33] S. K. Soni, B. Thomas, V. R. Kar, *Mater. Tod. Commun.* **2020**, *25*, 101546.
- [34] J. Karger-Kocsis, H. Mahmood, A. Pegoretti, *Compos. Sci. Technol.* **2020**, *186*, 107932.
- [35] P. Y. Hung, K. T. Lau, B. Fox, N. Hameed, J. H. Lee, D. Hui, *Composites, Part B* **2018**, *133*, 240.
- [36] F. S. Da Luz, F. D. C. Garcia Filho, M. T. G. Del-Río, L. F. C. Nascimento, W. A. Pinheiro, S. N. Monteiro, *Polymers* **2020**, *12*, 1601.
- [37] D. Rajak, D. Pagar, P. Menezes, E. Linul, *Polymers* **2019**, *11*, 1667.
- [38] S. Yentl, G. Larissa, V. Ignaas, *Composites, Part A* **2014**, *67*, 181.
- [39] J. D. H. Hughes, *Compos. Sci. Technol.* **1991**, *41*, 13.
- [40] Y. Zhou, M. Fan, L. Chen, *Composites, Part B* **2016**, *101*, 31.
- [41] W. T. Y. Tze, D. J. Gardner, C. P. Tripp, S. C. O'Neill, *J. Adhesion Sci. Technol.* **2006**, *20*, 1649.
- [42] S. Demiroglu, V. Singaravelu, M. Ö. Seydibeyoğlu, M. Misra, A. K. Mohanty, in *Fiber Technology for Fiber-Reinforced Composites* (Eds: M. Ö. Seydibeyoğlu, A. K. Mohanty, M. Misra), Woodhead Publishing, London, UK **2017**, p. 277.
- [43] Y. Tian, H. Zhang, Z. Zhang, *Composites, Part A* **2017**, *98*, 1.
- [44] L. Yan, N. Chouh, K. Jayaraman, *Composites, Part B* **2014**, *56*, 296.
- [45] B. G. Cho, S. H. Hwang, M. Park, J. K. Park, Y. B. Park, H. G. Chae, *Composites, Part B* **2019**, *160*, 436.
- [46] Y. Kusano, H. Mortensen, B. Stenum, P. Kingshott, T. L. Andersen, P. Brøndsted, J. B. Bilde-Sørensen, B. F. Sørensen, H. Bindsvlev, *Plasma Processes Polym.* **2007**, *4*, S455.
- [47] P. Compston, J. Schiemer, A. Cvetanovska, *Compos. Struct.* **2008**, *86*, 22.
- [48] W. K. Ng, M. Johar, H. A. Israr, K. J. Wong, in *Interfaces in Particle and Fiber Reinforced Composites* (Eds: K. L. Goh, M. K. Awasthi, R. T. De Silva, S. Thomas), Woodhead Publishing, **2020**, p. 163.
- [49] X. Zhang, X. Fan, C. Yan, H. Li, Y. Zhu, X. Li, L. Yu, *ACS Appl. Mater. Interf.* **2012**, *4*, 1543.
- [50] X. Cheng, T. Yokozeki, L. Wu, H. Wang, J. M. Zhang, J. Koyanagi, Z. Weng, Q. Sun, *Composites, Part A* **2016**, *90*, 243.
- [51] W. Qin, F. Vautard, L. T. Drzal, J. Yu, *Composites, Part B* **2015**, *69*, 335.
- [52] X. Shen, J. Jia, C. Chen, Y. Li, J. K. Kim, *J. Mater. Sci.* **2014**, *49*, 3225.
- [53] V. C. S. Chandrasekaran, S. G. Advani, M. H. Santare, *Composites, Part A* **2011**, *42*, 1007.
- [54] C.-Y. Dang, B.-L. Tang, X.-L. Zeng, J. Xu, M.-J. Feng, Y. Jiang, X.-J. Shen, *Mater. Res. Express* **2019**, *6*, 085324.
- [55] B. Gao, R. Zhang, M. He, L. Sun, C. Wang, L. Liu, L. Zhao, H. Cui, A. Cao, *Composites, Part A* **2016**, *90*, 433.
- [56] A. Godara, L. Gorbatikh, G. Kalinka, A. Warriar, O. Rochez, L. Mezzo, F. Luizi, A. W. van Vuure, S. V. Lomov, I. Verpoest, *Compos. Sci. Technol.* **2010**, *70*, 1346.
- [57] A. F. Avila, D. T. S. Morais, *Compos. Sci. Technol.* **2005**, *65*, 827.
- [58] S. M. R. Kazmi, Q. Govignon, S. Bickerton, *J. Compos. Mater.* **2019**, *53*, 327.
- [59] M. R. Ricciardi, V. Antonucci, M. Durante, M. Giordano, L. Nele, G. Starace, A. Langella, *J. Compos. Mater.* **2013**, *48*, 1365.
- [60] R. Balint, N. J. Cassidy, S. H. Cartmell, *Acta Biomater.* **2014**, *10*, 2341.
- [61] S. H. Han, E. J. Cho, H. C. Lee, K. Jeong, S. S. Kim, *Compos. Struct.* **2015**, *119*, 50.
- [62] Y. Rachmadini, V. B. C. Tan, T. E. Tay, *J. Reinf. Plast. Compos.* **2010**, *29*, 2782.
- [63] M. A. Yalcinkaya, E. M. Sozer, M. C. Altan, *Composites, Part A* **2017**, *102*, 336.
- [64] O. P. L. McGregor, M. Duhovic, A. A. Somashekar, D. Bhattacharyya, *Composites, Part A* **2017**, *101*, 59.
- [65] P. Mertiny, F. Ellyin, A. Hothan, *Compos. Sci. Technol.* **2004**, *64*, 1.
- [66] A. H. Miller, N. Dodds, J. M. Hale, A. G. Gibson, *Composites, Part A* **1998**, *29*, 773.
- [67] M. D. Wakeman, T. A. Cain, C. D. Rudd, R. Brooks, A. C. Long, *Compos. Sci. Technol.* **1998**, *58*, 1879.
- [68] E. Oromiehie, B. G. Prusty, P. Compston, G. Rajan, *Compos. Struct.* **2019**, *224*, 110987.

- [69] S. Y. Park, C. H. Choi, W. J. Choi, S. S. Hwang, *Appl. Compos. Mater.* **2019**, 26, 187.
- [70] A. A. Khan, A. A. Al-Kheraif, A. M. Al-Shehri, E. Säilynoja, P. K. Vallittu, *J. Mech. Behav. Biomed. Mater.* **2018**, 78, 414.
- [71] T. Centea, L. K. Grunenfelder, S. R. Nutt, *Composites, Part A* **2015**, 70, 132.
- [72] L. Zhang, X. Wang, J. Pei, Y. Zhou, *J. Mater. Sci.* **2020**, 55, 7121.
- [73] S. Geller, K. Holeczek, A. Winkler, T. Tyczynski, T. Weber, M. Gude, N. Modler, in *Performance Testing of Textiles* (Ed: L. Wang), Woodhead Publishing, London, UK **2016**, 155.
- [74] F. Valorosi, E. De Meo, T. Blanco-Varela, B. Martorana, A. Veca, N. Pugno, I. A. Kinloch, G. Anagnostopoulos, C. Galiotis, F. Bertocchi, J. Gomez, E. Treossi, R. J. Young, V. Palermo, *Compos. Sci. Technol.* **2020**, 185, 107848.
- [75] A. Lonjon, P. Demont, E. Dantras, C. Lacabanne, *J. Non-Cryst. Solids* **2012**, 358, 1859.
- [76] S. Chen, Y. Feng, M. Qin, T. Ji, W. Feng, *Carbon* **2017**, 116, 84.
- [77] J. R. N. Gnidakouong, J.-H. Kim, H. Kim, Y.-B. Park, *Mater. Sci. Eng., B* **2019**, 248, 114403.
- [78] H. Zhang, E. Bilotti, T. Peijs, *Nanocomposites* **2015**, 1, 167.
- [79] S. Boztepe, H. Liu, D. Heider, E. T. Thostenson, *Compos. Struct.* **2018**, 189, 340.
- [80] J. Zhang, R. Zhuang, J. Liu, E. Mäder, G. Heinrich, S. Gao, *Carbon* **2010**, 48, 2273.
- [81] B. Wang, Y. Duan, Z. Xin, X. Yao, D. Abliz, G. Ziegmann, *Compos. Sci. Technol.* **2018**, 158, 51.
- [82] G. Fredi, S. Jeschke, A. Boulaoued, J. Wallenstein, M. Rashidi, F. Liu, R. Harnden, D. Zenkert, J. Hagberg, G. Lindbergh, *Multi-funct. Mater.* **2018**, 1, 015003.
- [83] B. G. Falzon, P. Robinson, S. Frenz, B. Gilbert, *Composites, Part A* **2015**, 68, 323.
- [84] P. Tran, Q. T. Nguyen, K. T. Lau, *Composites, Part B* **2018**, 155, 31.
- [85] F. Bonaccorso, A. Lombardo, T. Hasan, Z. Sun, L. Colombo, A. C. Ferrari, *Mater. Today* **2012**, 15, 564.
- [86] W. Yang, C. Wang, *J. Mater. Chem. C* **2016**, 4, 7193.
- [87] X. Dong, B. Li, A. Wei, X. Cao, M. B. Chan-Park, H. Zhang, L.-J. Li, W. Huang, P. Chen, *Carbon* **2011**, 49, 2944.
- [88] Y. Wang, X. Xu, J. Lu, M. Lin, Q. Bao, B. Ozyilmaz, K. P. Loh, *ACS Nano* **2010**, 4, 6146.
- [89] F. Bonaccorso, A. Bartolotta, J. N. Coleman, C. Backes, *Adv. Mater.* **2016**, 28, 6136.
- [90] Y. Hernandez, V. Nicolosi, M. Lotya, F. M. Blighe, Z. Sun, S. De, I. McGovern, B. Holland, M. Byrne, Y. K. Gun'Ko, *Nat. Nanotechnol.* **2008**, 3, 563.
- [91] V. Nicolosi, M. Chhowalla, M. G. Kanatzidis, M. S. Strano, J. N. Coleman, *Science* **2013**, 340, 1226419.
- [92] J. Hassoun, F. Bonaccorso, M. Agostini, M. Angelucci, M. G. Betti, R. Cingolani, M. Gemmi, C. Mariani, S. Panero, V. Pellegrini, *Nano Lett.* **2014**, 14, 4901.
- [93] P. Blake, P. D. Brimicombe, R. R. Nair, T. J. Booth, D. Jiang, F. Schedin, L. A. Ponomarenko, S. V. Morozov, H. F. Gleeson, E. W. Hill, *Nano Lett.* **2008**, 8, 1704.
- [94] T. Hasan, F. Torrisi, Z. Sun, D. Popa, V. Nicolosi, G. Privitera, F. Bonaccorso, A. Ferrari, *Phys. Stat. Sol.* **2010**, 247, 2953.
- [95] U. Khan, A. O'Neill, M. Lotya, S. De, J. N. Coleman, *Small* **2010**, 6, 864.
- [96] M. Lotya, Y. Hernandez, P. J. King, R. J. Smith, V. Nicolosi, L. S. Karlsson, F. M. Blighe, S. De, Z. Wang, I. McGovern, *J. Am. Chem. Soc.* **2009**, 131, 3611.
- [97] O. M. Maragó, F. Bonaccorso, R. Saija, G. Privitera, P. G. Gucciardi, M. A. Iatì, G. Calogero, P. H. Jones, F. Borghese, P. Denti, *ACS Nano* **2010**, 4, 7515.
- [98] M. Buzaglo, M. Shtein, O. Regev, *Chem. Mater.* **2016**, 28, 21.
- [99] T. Panagiotou, S. Mesite, J. Bernard, K. Chomistek, R. Fisher, *Nanotech. Conf. Trade Show* **2008**, 1, 688.
- [100] T. Lajunen, K. Hisazumi, T. Kanazawa, H. Okada, Y. Seta, M. Yliperttula, A. Urtti, Y. Takashima, *Eur. J. Pharm. Sci.* **2014**, 62, 23.
- [101] S. Y. Tang, P. Shridharan, M. Sivakumar, *Ultrason. Sonochem.* **2013**, 20, 485.
- [102] S. M. Jafari, Y. He, B. Bhandari, *J. Food Eng.* **2007**, 82, 478.
- [103] T. Panagiotou, J. M. Bernard, S. V. Mesite, presented at *Nano Sci. Tech. Inst. (NSTI) Conf. Expo Proc.* **2008**, 1, 39.
- [104] P. G. Karagiannidis, S. A. Hodge, L. Lombardi, F. Tomarchio, N. Decorde, S. Milana, I. Goykhman, Y. Su, S. V. Mesite, D. N. Johnstone, *ACS Nano* **2017**, 11, 2742.
- [105] W. J. Hyun, E. B. Secor, M. C. Hersam, C. D. Frisbie, L. F. Francis, *Adv. Mater.* **2015**, 27, 109.
- [106] E. B. Secor, P. L. Prabhurashi, K. Puntambekar, M. L. Geier, M. C. Hersam, *J. Phys. Chem. Lett.* **2013**, 4, 1347.
- [107] E. L. Paul, V. A. Atiemo-Obeng, S. M. Kresta, *Handbook of Industrial Mixing: Science and Practice*, John Wiley & Sons, Hoboken, NJ **2003**.
- [108] J. Wang, K. K. Manga, Q. Bao, K. P. Loh, *J. Am. Chem. Soc.* **2011**, 133, 8888.
- [109] C.-S. Lee, S. J. Shim, T. H. Kim, *Nanomaterials* **2020**, 10, 267.
- [110] D. Li, M. B. Müller, S. Gilje, R. B. Kaner, G. G. Wallace, *Nat. Nanotechnol.* **2008**, 3, 101.
- [111] J. Liu, J. Tang, J. J. Gooding, *J. Mater. Chem.* **2012**, 22, 12435.
- [112] S. P. Lonkar, Y. S. Deshmukh, A. A. Abdala, *Nano Res.* **2015**, 8, 1039.
- [113] N. Karim, S. Afroj, D. Leech, A. M. Abdelkader, *Oxide Electronics* **2021**, 21, 21.
- [114] S. Pei, H.-M. Cheng, *Carbon* **2012**, 50, 3210.
- [115] J.-P. Salvetat-Delmotte, A. Rubio, *Carbon* **2002**, 40, 1729.
- [116] S. Mallakpour, S. Rashidimoghadam, *Composite Nanoadsorbents*, Elsevier, **2019**, p. 211.
- [117] S. Imtiaz, M. Siddiq, A. Kausar, S. T. Muntha, J. Ambreen, I. Bibi, *Chin. J. Polym. Sci.* **2018**, 36, 445.
- [118] M. Dresselhaus, G. Dresselhaus, P. Eklund, R. Saito, M. S. Dresselhaus, G. Dresselhaus, *Physical*, Academic Press, San Diego **1996**.
- [119] H. Dai, *Acc. Chem. Res.* **2002**, 35, 1035.
- [120] H. Dai, *Carbon Nanotubes* **2001**, 80, 29.
- [121] J. P. Gore, A. Sane, *Carbon Nanotubes-Synth. Characteri. Appl.* **2011**, 1, 16801.
- [122] J. Kong, H. T. Soh, A. M. Cassell, C. F. Quate, H. Dai, *Nature* **1998**, 395, 878.
- [123] J. H. Hafner, M. J. Bronikowski, B. R. Azamian, P. Nikolaev, A. G. Rinzler, D. T. Colbert, K. A. Smith, R. E. Smalley, *Chem. Phys. Lett.* **1998**, 296, 195.
- [124] B. Satishkumar, A. Govindaraj, R. Sen, C. Rao, *Chem. Phys. Lett.* **1998**, 293, 47.
- [125] P. Nikolaev, M. J. Bronikowski, R. K. Bradley, F. Rohmund, D. T. Colbert, K. Smith, R. E. Smalley, *Chem. Phys. Lett.* **1999**, 313, 91.
- [126] M. Su, B. Zheng, J. Liu, *Chem. Phys. Lett.* **2000**, 322, 321.
- [127] J.-F. Colomer, C. Stephan, S. Lefrant, G. Van Tendeloo, I. Willems, Z. Konya, A. Fonseca, C. Laurent, J. B. Nagy, *Chem. Phys. Lett.* **2000**, 317, 83.
- [128] C. Journet, W. Maser, P. Bernier, A. Loiseau, M. L. de La Chapelle, D. S. Lefrant, P. Deniard, R. Lee, J. Fischer, *Nature* **1997**, 388, 756.
- [129] A. Thess, R. Lee, P. Nikolaev, H. Dai, P. Petit, J. Robert, C. Xu, Y. H. Lee, S. G. Kim, A. G. Rinzler, *Science* **1996**, 273, 483.
- [130] H. Zhang, Y. Liu, M. Kuwata, E. Bilotti, T. Peijs, *Composites, Part A* **2015**, 70, 102.

- [131] R. K. Prusty, S. K. Ghosh, D. K. Rathore, B. C. Ray, *Composites, Part A* **2017**, 95, 40.
- [132] M. Raífee, F. Nitzsche, J. Laliberte, S. Hind, F. Robitaille, M. R. Labrosse, *Composites, Part B* **2019**, 164, 1.
- [133] Y. J. Kwon, Y. Kim, H. Jeon, S. Cho, W. Lee, J. U. Lee, *Composites, Part B* **2017**, 122, 23.
- [134] R. Moriche, M. Sánchez, A. Jiménez-Suárez, S. G. Prolongo, A. Ureña, *Composites, Part B* **2016**, 98, 49.
- [135] L. Gao, T.-W. Chou, E. T. Thostenson, Z. Zhang, M. Coulaud, *Carbon* **2011**, 49, 3382.
- [136] M. S. Chen, S. M. Goh, K. Yang, A. A. Nikitina, S. Y. Chen, X. Y. Leng, N. Karim, L. Hanson, H. F. Gleeson, K. S. Novoselov, D. V. Andreeva, *Adv. Mater. Interfaces* **2021**, 8, 2101432.
- [137] Z. L. Chen, K. Yang, T. F. Xian, C. Kocabas, S. V. Morozov, A. H. C. Neto, K. S. Novoselov, D. V. Andreeva, M. Koperski, *ACS Appl. Mater. Interfaces* **2021**, 13, 27278.
- [138] R. Balaji, M. Sasikumar, *Composites, Part A* **2017**, 103, 48.
- [139] N. Karim, M. Zhang, S. Afroj, V. Koncherry, P. Potluri, K. S. Novoselov, *RSC Adv.* **2018**, 8, 16815.
- [140] R. Moriche, A. Jiménez-Suárez, M. Sánchez, S. G. Prolongo, A. Ureña, *Compos. Sci. Technol.* **2017**, 146, 59.
- [141] S. Bhattacharjee, C. R. Macintyre, P. Bahl, U. Kumar, X. Wen, K. F. Aguey-Zinsou, A. A. Chughtai, R. Joshi, *Adv. Mater. Interfaces* **2020**, 7, 2000814.
- [142] C. Cao, Z. Lin, X. Liu, Y. Jia, E. Saiz, S. E. Wolf, H. D. Wagner, L. Jiang, Q. Cheng, *Adv. Funct. Mater.* **2021**, 31, 2102923.
- [143] A. Chavez-Valdez, M. S. P. Shaffer, A. R. Boccaccini, *J. Phys. Chem. B* **2013**, 117, 1502.
- [144] J. Chen, J. Wu, H. Ge, D. Zhao, C. Liu, X. Hong, *Composites, Part A* **2016**, 82, 141.
- [145] P. He, B. Huang, L. Liu, Q. Huang, T. Chen, *Polym. Compos.* **2016**, 37, 1515.
- [146] M. F. De Riccardis, D. Carbone, T. D. Makris, R. Giorgi, N. Lisi, E. Salernitano, *Carbon* **2006**, 44, 671.
- [147] N. Karim, S. Afroj, S. Tan, P. He, A. Fernando, C. Carr, K. S. Novoselov, *ACS Nano* **2017**, 11, 12266.
- [148] M. S. Sadi, J. Pan, A. Xu, D. Cheng, G. Cai, X. Wang, *Cellulose* **2019**, 26, 7569.
- [149] S. Afroj, M. H. Islam, N. Karim, *Multidiscipl. Dig. Publ. Inst. Proc.* **2021**, 68, 11.
- [150] M. Sharma, S. Gao, E. Mäder, H. Sharma, L. Y. Wei, J. Bijwe, *Compos. Sci. Technol.* **2014**, 102, 35.
- [151] J. Guo, C. Lu, F. An, S. He, *Mater. Lett.* **2012**, 66, 382.
- [152] R. L. Zhang, B. Gao, Q. H. Ma, J. Zhang, H. Z. Cui, L. Liu, *Mater. Des.* **2016**, 93, 364.
- [153] E. J. Garcia, B. L. Wardle, A. J. Hart, *Composites, Part A* **2008**, 39, 1065.
- [154] S. Zeng, M. Shen, S. Chen, L. Yang, F. Lu, Y. Xue, *Text. Res. J.* **2019**, 89, 2353.
- [155] C. Cao, J. Peng, X. Liang, E. Saiz, S. E. Wolf, H. D. Wagner, L. Jiang, Q. Cheng, *Composites, Part A* **2021**, 140, 106161.
- [156] S. Xiong, Y. Zhao, Y. Wang, J. Song, X. Zhao, S. Li, *Appl. Surf. Sci.* **2021**, 546, 149135.
- [157] Y. Peng, D. Huang, *Appl. Surf. Sci.* **2013**, 283, 81.
- [158] Y. Lin, J. Jin, O. Kusmartsevab, M. Song, *J. Phys. Chem. C* **2013**, 117, 17237.
- [159] H. Mahmood, M. Tripathi, N. Pugno, A. Pegoretti, *Compos. Sci. Technol.* **2016**, 126, 149.
- [160] M. Diba, A. García-Gallastegui, R. N. Klupp Taylor, F. Pishbin, M. P. Ryan, M. S. P. Shaffer, A. R. Boccaccini, *Carbon* **2014**, 67, 656.
- [161] C. Deng, J. Jiang, F. Liu, L. Fang, J. Wang, D. Li, J. Wu, *Surf. Coat. Technol.* **2015**, 272, 176.
- [162] E. Bekyarova, E. T. Thostenson, A. Yu, H. Kim, J. Gao, J. Tang, H. T. Hahn, T. W. Chou, M. E. Itkis, R. C. Haddon, *Langmuir* **2007**, 23, 3970.
- [163] F. Wang, X. Cai, *J. Mater. Sci.* **2019**, 54, 3847.
- [164] C. Xiang, W. Lu, Y. Zhu, Z. Sun, Z. Yan, C. C. Hwang, J. M. Tour, *ACS Appl. Mater. Interf.* **2012**, 4, 131.
- [165] H. Yao, G. Zhou, W. Wang, M. Peng, *Compos. Struct.* **2018**, 195, 288.
- [166] W. Wang, G. Xian, H. Li, *Cellulose* **2019**, 26, 8165.
- [167] K. Patel, P. Potluri, Z. Yousaf, A. Wilkinson, *Composites, Part B* **2019**, 165, 109.
- [168] L. Tzounis, M. Zappalorto, F. Panozzo, K. Tsirka, L. Maragoni, A. S. Paipetis, M. Quaresimin, *Composites, Part B* **2019**, 169, 37.
- [169] J. Chen, D. Zhao, X. Jin, C. Wang, D. Wang, H. Ge, *Compos. Sci. Technol.* **2014**, 97, 41.
- [170] L. Zeng, X. Liu, X. Chen, C. Soutis, *Appl. Compos. Mater.* **2018**, 25, 843.
- [171] Y. Li, Q. Peng, X. He, P. Hu, C. Wang, Y. Shang, R. Wang, W. Jiao, H. Lv, *J. Mater. Chem.* **2012**, 22, 18748.
- [172] E. Piccinini, C. Bliem, J. M. Giussi, W. Knoll, O. Azzaroni, *Langmuir* **2019**, 35, 8038.
- [173] L. H. Hess, A. Lyuleeva, B. M. Blaschke, M. Sachsenhauser, M. Seifert, J. A. Garrido, F. Deubel, *ACS Appl. Mater. Interfaces* **2014**, 6, 9705.
- [174] S. J. Ling, Q. Wang, D. Zhang, Y. Y. Zhang, X. Mu, D. L. Kaplan, M. J. Buehler, *Adv. Funct. Mater.* **2018**, 28, 1705291.
- [175] T. W. Ebbesen, P. M. Ajayan, *Nature* **1992**, 358, 220.
- [176] A. Thess, R. Lee, P. Nikolaev, H. Dai, P. Petit, J. Robert, C. Xu, Y. H. Lee, S. G. Kim, A. G. Rinzler, D. T. Colbert, G. E. Scuseria, D. Tománek, J. E. Fischer, R. E. Smalley, *Science* **1996**, 273, 483.
- [177] M. Endo, K. Takeuchi, K. Kobori, K. Takahashi, H. W. Kroto, A. Sarkar, *Carbon* **1995**, 33, 873.
- [178] Q. Song, K.-z. Li, H.-l. Li, H.-j. Li, C. Ren, *Carbon* **2012**, 50, 3949.
- [179] S. Zhu, C. H. Su, S. L. Lehoczyk, I. Muntele, D. Ila, *Diamond Relat. Mater.* **2003**, 12, 1825.
- [180] T. R. Pozegic, J. V. Anguita, I. Hamerton, K. D. G. I. Jayawardena, J. S. Chen, V. Stolojan, P. Balocchi, R. Walsh, S. R. P. Silva, *Sci. Rep.* **2016**, 6, 37334.
- [181] Q. Zhang, J. Liu, R. Sager, L. Dai, J. Baur, *Compos. Sci. Technol.* **2009**, 69, 594.
- [182] Z. F. Ren, Z. P. Huang, *Science* **1998**, 282, 1105.
- [183] V. P. Veedu, A. Cao, X. Li, K. Ma, C. Soldano, S. Kar, P. M. Ajayan, M. N. Ghasemi-Nejhad, *Nat. Mater.* **2006**, 5, 457.
- [184] H. Qian, A. Bismarck, E. S. Greenhalgh, G. Kalinka, M. S. P. Shaffer, *Chem. Mater.* **2008**, 20, 1862.
- [185] R. J. Sager, P. J. Klein, D. C. Lagoudas, Q. Zhang, J. Liu, L. Dai, J. W. Baur, *Compos. Sci. Technol.* **2009**, 69, 898.
- [186] K. Yildiz, İ. Gürkan, F. Turgut, F. Cebeci, H. Cebeci, *Compos. Commun.* **2020**, 21, 100423.
- [187] G. Hu, J. Kang, L. W. Ng, X. Zhu, R. C. Howe, C. G. Jones, M. C. Hersam, T. Hasan, *Chem. Soc. Rev.* **2018**, 47, 3265.
- [188] N. Karim, S. Afroj, A. Malandraki, S. Butterworth, C. Beach, M. Rigout, K. S. Novoselov, A. J. Casson, S. G. Yeates, *J. Mater. Chem. C* **2017**, 5, 11640.
- [189] M. R. Islam, S. Afroj, C. Beach, M. H. Islam, C. Parraman, A. Abdelkader, A. J. Casson, K. S. Novoselov, N. Karim, *iScience* **2022**, 25, 103945.
- [190] H. Zhou, W. Qin, Q. Yu, H. Cheng, X. Yu, H. Wu, *Nanomaterials* **2019**, 9, 283.
- [191] L. Groo, J. Nasser, L. Zhang, K. Steinke, D. Inman, H. Sodano, *Compos. Sci. Technol.* **2020**, 199, 108367.
- [192] C. Soutis, *Mater. Sci. Eng., A* **2005**, 412, 171.
- [193] M. G. Callens, L. Gorbatikh, I. Verpoest, *Composites, Part A* **2014**, 61, 235.

- [194] K. W. Garrett, J. E. Bailey, *J. Mater. Sci.* **1977**, 12, 2189.
- [195] A. Gopinath, M. S. Kumar, A. Elayaperumal, *Proc. Eng.* **2014**, 97, 2052.
- [196] K. A. Imran, K. N. Shivakumar, *J. Compos. Mater.* **2019**, 53, 93.
- [197] B. Zhang, R. Asmatulu, S. A. Soltani, L. N. Le, S. S. A. Kumar, *J. Appl. Polym. Sci.* **2014**, 131, 40286.
- [198] E. F. Reia Da Costa, A. A. Skordos, I. K. Partridge, A. Rezai, *Composites, Part A* **2012**, 43, 593.
- [199] Z. Fan, S. G. Advani, *J. Nanosci. Nanotechnol.* **2008**, 8, 1669.
- [200] Z. Fan, K. T. Hsiao, S. G. Advani, *Carbon* **2004**, 42, 871.
- [201] A. Surnova, D. Balkaev, D. Musin, R. Amirov, A. M. Dimiev, *Composites, Part B* **2019**, 162, 685.
- [202] W. Li, A. Dichiaro, J. Bai, *Compos. Sci. Technol.* **2013**, 74, 221.
- [203] A. Liang, X. Jiang, X. Hong, Y. Jiang, Z. Shao, D. Zhu, *Coatings* **2018**, 8, 33.
- [204] K. Lu, R. Lago, Y. Chen, M. Green, P. Harris, S. Tsang, *Carbon* **1996**, 34, 814.
- [205] E. Mannov, H. Schmutzler, S. Chandrasekaran, C. Viets, S. Buschhorn, F. Tölle, R. Mülhaupt, K. Schulte, *Compos. Sci. Technol.* **2013**, 87, 36.
- [206] F. H. Gojny, M. H. G. Wichmann, U. Köpke, B. Fiedler, K. Schulte, *Compos. Sci. Technol.* **2004**, 64, 2363.
- [207] I. El Sawi, P. A. Olivier, P. Demont, H. Bougherara, *Compos. Sci. Technol.* **2012**, 73, 19.
- [208] B. Alemour, O. Badran, M. R. Hassan, *J. Aerosp. Technol. Manag.* **2019**, 11, e1919.
- [209] E. Kandare, A. A. Khatibi, S. Yoo, R. Wang, J. Ma, P. Olivier, N. Gleizes, C. H. Wang, *Composites, Part A* **2015**, 69, 72.
- [210] M. Gagné, D. Therriault, *Prog. Aerosp. Sci.* **2014**, 64, 1.
- [211] H. Xu, X. Tong, Y. Zhang, Q. Li, W. Lu, *Compos. Sci. Technol.* **2016**, 127, 113.
- [212] D. He, B. Fan, H. Zhao, X. Lu, M. Yang, Y. Liu, J. Bai, *ACS App. Mater. Interf.* **2017**, 9, 2948.
- [213] E. C. Senis, I. O. Golosnoy, T. Andritsch, J. M. Dulieu-Barton, O. T. Thomsen, *Polym. Compos.* **2020**, 41, 3510.
- [214] B. Ashrafi, A. M. Díez-Pascual, L. Johnson, M. Genest, S. Hind, Y. Martínez-Rubi, J. M. González-Domínguez, M. T. Martínez, B. Simard, M. A. Gómez-Fatou, A. Johnston, *Composites, Part A* **2012**, 43, 1267.
- [215] J. Wu, J. Chen, Y. Zhao, W. Liu, W. Zhang, *Composites, Part B* **2016**, 105, 167.
- [216] S. Wang, R. Downes, C. Young, D. Haldane, A. Hao, R. Liang, B. Wang, C. Zhang, R. Maskell, *Adv. Eng. Mater.* **2015**, 17, 1442.
- [217] E. C. Senis, I. O. Golosnoy, J. M. Dulieu-Barton, O. T. Thomsen, *J. Mater. Sci.* **2019**, 54, 8955.
- [218] N. Burger, A. Laachachi, M. Ferriol, M. Lutz, V. Toniazzo, D. Ruch, *Prog. Polym. Sci.* **2016**, 61, 1.
- [219] C. Huang, X. Qian, R. Yang, *Mater. Sci. Eng.: R: Rep.* **2018**, 132, 1.
- [220] S. H. Noh, W. Eom, W. J. Lee, H. Park, S. B. Ambade, S. O. Kim, T. H. Han, *Carbon* **2019**, 142, 230.
- [221] J. Li, Z. Wu, C. Huang, L. Li, *Compos. Sci. Technol.* **2014**, 104, 81.
- [222] S. Wang, J. Qiu, *Composites, Part B* **2010**, 41, 533.
- [223] A. M. Díez-Pascual, B. Ashrafi, M. Naffakh, J. M. González-Domínguez, A. Johnston, B. Simard, M. T. Martínez, M. A. Gómez-Fatou, *Carbon* **2011**, 49, 2817.
- [224] Z. Shen, S. Bateman, D. Y. Wu, P. McMahon, M. Dell'Olivo, J. Gotama, *Compos. Sci. Technol.* **2009**, 69, 239.
- [225] Y. C. Shin, E. Novin, H. Kim, *Int. J. Precis. Eng. Manuf.* **2015**, 16, 465.
- [226] X. Fu, C. Zhang, T. Liu, R. Liang, B. Wang, *Nanotechnology* **2010**, 21, 235701.
- [227] G. Zhao, H.-Y. Liu, X. Du, H. Zhou, Z. Pan, Y.-W. Mai, Y.-Y. Jia, W. Yan, *Composites, Part B* **2020**, 198, 108249.
- [228] F. Li, Y. Liu, C. B. Qu, H. M. Xiao, Y. Hua, G. X. Sui, S. Y. Fu, *Polymer* **2015**, 59, 155.
- [229] G. V. Seretis, I. D. Theodorakopoulos, D. E. Manolagos, C. G. Provatidis, *Composites, Part B* **2018**, 147, 33.
- [230] S. P. Sharma, S. C. Lakkad, *Composites, Part A* **2011**, 42, 8.
- [231] A. Dilfi K F, Z. Che, G. Xian, *J. Nat. Fibers* **2019**, 16, 388.
- [232] M. Kamaraj, E. A. Dodson, S. Datta, *Adv. Compos. Mater.* **2020**, 29, 443.
- [233] H. Mei, S. Zhang, H. Chen, H. Zhou, X. Zhai, L. Cheng, *Compos. Sci. Technol.* **2016**, 134, 89.
- [234] H. Wang, L. Yang, H. Guo, Y. Zhao, J. Zhao, *Fibers Polym.* **2019**, 20, 1266.
- [235] J. Bahador Dastorian, H. Soraya, R. Saeed, R. Suraya Abdul, B. M. Sa'Ari, B. Sepideh Keshan, *J. Nanomater.* **2015**, 149736.
- [236] M. H. Islam, M. R. Islam, M. Dulal, S. Afroj, N. Karim, *iScience* **2022**, 25, 103597.
- [237] H. Yaghoobi, A. Fereidoon, *Composites, Part B* **2019**, 162, 314.
- [238] C. Wang, J. Li, S. Sun, X. Li, F. Zhao, B. Jiang, Y. Huang, *Compos. Sci. Technol.* **2016**, 135, 46.
- [239] L. Ma, Y. Zhu, P. Feng, G. Song, Y. Huang, H. Liu, J. Zhang, J. Fan, H. Hou, Z. Guo, *Composites, Part B* **2019**, 176, 107078.
- [240] X. Wang, C. Li, Y. Chi, M. Piao, J. Chu, H. Zhang, Z. Li, W. Wei, *Nanomaterials* **2018**, 8, 414.
- [241] W. Qin, C. Chen, J. Zhou, J. Meng, *Materials* **2020**, 13, 1457.
- [242] Y. Li, S. Wang, Q. Wang, M. Xing, *Composites, Part B* **2018**, 133, 35.
- [243] W. Qin, F. Vautard, L. T. Drzal, J. Yu, *Polym. Compos.* **2016**, 37, 1549.
- [244] H. Mahmood, L. Vanzetti, M. Bersani, A. Pegoretti, *Composites, Part A* **2018**, 107, 112.
- [245] C. Deng, J. Jiang, F. Liu, L. Fang, J. Wang, D. Li, J. Wu, *J. Mater. Sci.* **2015**, 50, 5886.
- [246] Y. Li, C. Chen, J. Xu, Z. Zhang, B. Yuan, X. Huang, *J. Mater. Sci.* **2015**, 50, 1117.
- [247] R. L. Zhang, B. Gao, W. T. Du, J. Zhang, H. Z. Cui, L. Liu, Q. H. Ma, C. G. Wang, F. H. Li, *Composites, Part A* **2016**, 84, 455.
- [248] W. Zhanjun, X. P. Qing, F.-K. Chang, *J. Intell. Mater. Syst. Struct.* **2009**, 20, 1069.
- [249] T. Clarke, F. Simonetti, S. Rohklin, P. Cawley, *IEEE Trans. Ultrason. Ferroelectr. Freq. Control.* **2009**, 56, 1457.
- [250] A. Hamdan, M. T. H. Sultan, F. Mustapha, *Structural Health Monitoring of Biocomposites, Fiber-Reinforced Composites and Hybrid Composites*, 1st ed., Woodhead Publishing Series in Composites Science and Engineering, Vol. 14, Woodhead Publishing, UK **2019**.
- [251] P. Khalili, P. Cawley, *IEEE Trans Ultrason Ferroelectr Freq Control.* **2018**, 65, 648.
- [252] B. Herdovics, F. Cegla, *Struct. Health Monit.: Int. J.* **2018**, 17, 24.
- [253] N. D. Alexopoulos, C. Bartholome, P. Poulin, Z. Marioli-Riga, *Compos. Sci. Technol.* **2010**, 70, 260.
- [254] J. Sebastian, N. Schehl, M. Bouchard, M. Boehle, L. Li, A. Lagounov, K. Lafdi, *Carbon* **2014**, 66, 191.
- [255] C. Rainieri, G. Fabbrocino, Y. Song, V. Shanov, *International Workshop Smart materials, structures & NTD in Aerospace conference, Canada* **2011**.
- [256] Y. Li, K. Wang, Q. Wang, J. Yang, P. Zhou, Y. Su, S. Guo, Z. Su, *Struct. Health Monit.* **2020**, 20, 240.
- [257] L. Gao, T. W. Chou, E. T. Thostenson, Z. Zhang, *Carbon* **2010**, 48, 3788.
- [258] K. M. Tripathi, F. Vincent, M. Castro, J. F. Feller, *Nanocomposites* **2016**, 2, 125.
- [259] R. C. Zhuang, T. T. L. Doan, J. W. Liu, J. Zhang, S. L. Gao, E. Mäder, *Carbon* **2011**, 49, 2683.
- [260] O. Fakorede, Z. Feger, H. Ibrahim, A. Ilinca, J. Perron, C. Masson, *Renew. Sust. Energy Rev.* **2016**, 65, 662.
- [261] S. Li, Y. Wang, X. Li, W. Wei, G. Zhao, P. He, presented at *2010 Int. Conf. Intell. Syst. Des. Eng. Appl.*, Changsha, China, October **2010**.

- [262] O. Parent, A. Ilinca, *Cold Reg. Sci. Technol.* **2011**, 65, 88.
- [263] S. K. Thomas, R. P. Cassoni, C. D. MacArthur, *J. Aircr.* **1996**, 33, 841.
- [264] Z. Goraj, presented at *24th Int. Congr. Aeronaut. Sci.*, Japan, August **2004**.
- [265] J. Gao, H. Guo, X. Wang, P. Wang, Y. Wei, Z. Wang, Y. Huang, B. Yang, *J. Cleaner Prod.* **2019**, 206, 1110.
- [266] F. Zangrossi, F. Xu, N. Warrior, P. Karapappas, X. Hou, *J. Compos. Mater.* **2020**, 54, 3457.
- [267] N. Dalili, A. Edrisy, R. Carriveau, *Renew. Sust. Energy Rev.* **2009**, 13, 428.
- [268] A.-T. Chien, S. Cho, Y. Joshi, S. Kumar, *Polymer* **2014**, 55, 6896.
- [269] A. Ahmed, M. A. Jalil, M. M. Hossain, M. Moniruzzaman, B. Adak, M. T. Islam, M. S. Parvez, S. Mukhopadhyay, *J. Mater. Chem. C* **2020**, 8, 16204.
- [270] M. O. Faruk, A. Ahmed, M. A. Jalil, M. T. Islam, B. Adak, M. M. Hossain, S. Mukhopadhyay, *Appl. Mater. Today* **2021**, 23, 101025.
- [271] N. J. Kanu, E. Gupta, U. K. Vates, G. K. Singh, *Composites, Part A* **2019**, 121, 474.
- [272] H. Chu, Z. Zhang, Y. Liu, J. Leng, *Carbon* **2014**, 66, 154.
- [273] M. Tarfaoui, A. El Moumen, M. Boehle, O. Shah, K. Lafdi, *J. Mater. Sci.* **2019**, 54, 1351.
- [274] T. Pereira, Z. Guo, S. Nieh, J. Arias, H. T. Hahn, *Compos. Sci. Technol.* **2008**, 68, 1935.
- [275] T. Pereira, G. Zhanhu, S. Nieh, J. Arias, H. T. Hahn, *J. Compos. Mater.* **2009**, 43, 549.
- [276] E. L. Wong, D. M. Baechle, K. Xu, R. H. Carter, J. F. Snyder, E. D. Wetzel, *Proc. SAMPE Baltimore*, MD, USA **2007**.
- [277] S. Ekstedt, M. Wysocki, L. E. Asp, *Plast., Rubber Compos.* **2010**, 39, 148.
- [278] M. Y. Park, J. H. Kim, D. K. Kim, C. G. Kim, *Fibers Polym.* **2018**, 19, 599.
- [279] M. Kaempgen, M. Lebert, S. Roth, M. Soehn, N. Nicoloso, *J. Power Sources* **2008**, 180, 755.
- [280] J. South, D. Baechle, C. Hilton, D. Deschepper, E. Wetzel, Report no. ARL-TR- 4400, Aberdeen Proving Ground MD, Army Research Laboratory, **2008**.
- [281] D. Yu, K. Goh, H. Wang, L. Wei, W. Jiang, Q. Zhang, L. Dai, Y. Chen, *Nat. Nanotechnol.* **2014**, 9, 555.
- [282] B. J. Mapleback, T. J. Simons, Y. Shekibi, K. Ghorbani, A. N. Rider, *Electrochim. Acta* **2020**, 331, 135233.
- [283] R. Reece, C. Lekakou, P. A. Smith, *ACS Appl. Mater. Interf.* **2020**, 12, 25683.
- [284] J. Zhao, J. Zhu, Y. Li, L. Wang, Y. Dong, Z. Jiang, C. Fan, Y. Cao, R. Sheng, A. Liu, S. Zhang, H. Song, D. Jia, Z. Fan, *ACS Appl. Mater. Interf.* **2020**, 12, 11669.
- [285] Q. Yang, L. Dong, C. Xu, F. Kang, *RSC Adv.* **2016**, 6, 12525.
- [286] E. Senokos, Y. Ou, J. J. Torres, F. Sket, C. González, R. Marcilla, J. J. Vilatela, *Sci. Rep.* **2018**, 8, 3407.
- [287] K.-Y. Chan, B. Jia, H. Lin, N. Hameed, J.-H. Lee, K.-T. Lau, *Compos. Struct.* **2018**, 188, 126.
- [288] T. Adam, G. Liao, J. Petersen, S. Geier, B. Finke, P. Wierach, A. Kwade, M. Wiedemann, *Energies* **2018**, 11, 335.
- [289] Y. Zhang, J. Peng, M. Li, E. Saiz, S. E. Wolf, Q. Cheng, *ACS Nano* **2018**, 12, 8901.
- [290] H. Yang, presented at *2020 IEEE Transport. Electrification Conf. Expo (ITEC) USA* June **2020**.
- [291] D. Carlstedt, L. E. Asp, *Composites, Part B* **2020**, 186, 107822.
- [292] P. Liu, E. Sherman, A. Jacobsen, *J. Power Sources* **2009**, 189, 646.
- [293] K. Moyer, C. Meng, B. Marshall, O. Assal, J. Eaves, D. Perez, R. Karkkainen, L. Roberson, C. L. Pint, *Energy Storage Mater.* **2020**, 24, 676.
- [294] L. F. Aval, M. Ghoranneviss, G. B. Pour, *Heliyon* **2018**, 4, e00862.
- [295] Q. Ke, J. Wang, *J. Materiom.* **2016**, 2, 37.
- [296] Y. Gao, *Nanoscale Res. Lett.* **2017**, 12, 387.
- [297] CORDIS EU Research Results, <https://cordis.europa.eu/project/id/2342236/reporting>.
- [298] N. Shirshova, H. Qian, M. Houllé, J. H. G. Steinke, A. R. J. Kucernak, Q. P. V. Fontana, E. S. Greenhalgh, A. Bismarck, M. S. P. Shaffer, *Faraday Discuss.* **2014**, 172, 81.
- [299] A. Ganguly, A. Karakassides, J. Benson, S. Hussain, P. Papakonstantinou, *ACS Appl. Energy Mater.* **2020**, 3, 4245.
- [300] G. P. Moriarty, J. N. Wheeler, C. Yu, J. C. Grunlan, *Carbon* **2012**, 50, 885.
- [301] L. Tzounis, T. Gärtner, M. Liebscher, P. Pötschke, M. Stamm, B. Voit, G. Heinrich, *Polymer* **2014**, 55, 5381.
- [302] L. Wang, X. Jia, D. Wang, G. Zhu, J. Li, *Synth. Met.* **2013**, 181, 79.
- [303] S. Han, D. D. L. Chung, *Carbon* **2013**, 52, 30.
- [304] L. Tzounis, M. Liebscher, A. Tzounis, E. Petinakis, A. S. Paipetis, E. Mäder, M. Stamm, *RSC Adv.* **2016**, 6, 55514.
- [305] D. H. Sung, G.-H. Kang, K. Kong, M. Kim, H. W. Park, Y.-B. Park, *Composites, Part B* **2016**, 92, 202.
- [306] S. Saq'An, A. M. Zihlif, S. R. Al-Ani, G. Ragosta, *J. Mater. Sci.: Mater. Electron.* **2008**, 19, 1079.
- [307] D. Kim, Y. Kim, K. Choi, J. C. Grunlan, C. Yu, *ACS Nano* **2010**, 4, 513.
- [308] F. Fu, L. Hu, in *Advanced High Strength Natural Fibre Composites in Construction* (Eds: M. Fan, F. Fu), Woodhead Publishing, London, UK, **2017**, 405.
- [309] K. Yanagi, R. Moriya, Y. Yomogida, T. Takenobu, Y. Naitoh, T. Ishida, H. Kataura, K. Matsuda, Y. Maniwa, *Adv. Mater.* **2011**, 23, 2811.
- [310] X. Sun, Z. Zhang, X. Lu, G. Guan, H. Li, H. Peng, *Angew. Chem.* **2013**, 125, 7930.
- [311] W. Wang, X. Sun, W. Wu, H. Peng, Y. Yu, *Angew. Chem.* **2012**, 124, 4722.
- [312] Y. Deng, S. Gao, J. Liu, U. Gohs, E. Mäder, G. Heinrich, *Mater. Horiz.* **2017**, 4, 389.
- [313] H. Peng, X. Sun, F. Cai, X. Chen, Y. Zhu, G. Liao, D. Chen, Q. Li, Y. Lu, Y. Zhu, Q. Jia, *Nat. Nanotechnol.* **2009**, 4, 738.
- [314] O. Rifaie-Graham, E. A. Apebende, L. K. Bast, N. Bruns, *Adv. Mater.* **2018**, 30, 1705483.
- [315] E. Ahmed, *JEC Group*, <http://www.jeccomposites.com/knowledge/international-composites-news/prototype-car-bumper-made-graphene-composite> (accessed: June 2022).
- [316] *Politics & Government Week* **2019**, 2227.
- [317] A. K. Mohanty, S. Vivekanandhan, J.-M. Pin, M. Misra, *Science* **2018**, 362, 536.
- [318] Y. G. Thyavihalli Girijappa, S. Mavinkere Rangappa, J. Parameswaranpillai, S. Siengchin, *Front. Mater.* **2019**, 6, 226.
- [319] M. A. Uddin, S. Afroj, T. Hasan, C. Carr, K. S. Novoselov, N. Karim, *Adv. Sust. Syst.* **2022**, 6, 2100176.
- [320] M. N. Karim, M. Rigout, S. G. Yeates, C. Carr, *Dyes Pigm.* **2014**, 103, 168.
- [321] M. N. Karim, S. Afroj, M. Rigout, S. G. Yeates, C. Carr, *J. Mater. Sci.* **2015**, 50, 4576.
- [322] R. Siakeng, M. Jawaid, H. Ariffin, S. M. Sapuan, M. Asim, N. Saba, *Polym. Compos.* **2019**, 40, 446.
- [323] G. Koronis, A. Silva, M. Fontul, *Composites, Part B* **2013**, 44, 120.
- [324] B. Fadeel, C. Bussy, S. Merino, E. Vázquez, E. Flahaut, F. Mouchet, L. Evariste, L. Gauthier, A. J. Koivisto, U. Vogel, C. Martín, L. G. Delogu, T. Buerki-Thurnherr, P. Wick, D. Beloin-Saint-Pierre, R. Hischier, M. Pelin, F. Candotto Carniel, M. Tretiach, F. Cesca, F. Benfenati, D. Scaini, L. Ballerini, K. Kostarelos, M. Prato, A. Bianco, *ACS Nano* **2018**, 12, 10582.
- [325] M. R. P. Elenchezian, V. Vadlamudi, R. Raihan, K. Reifsnider, *Smart Mater. Struct.* **2021**, 30, 083001.
- [326] C. Gomez, A. Guardia, J. Mantari, A. Coronado, J. Reddy, *Mech. Adv. Mater. Struct.* **2022**, 29, 3076.



Mohammad Hamidul Islam is a Research Fellow at the Centre for Print Research (CFPR), UWE Bristol. He is currently investigating graphene-based technologies aimed at developing scalable and cost-effective natural and synthetic fiber smart composites and wearable smart textiles. Prior to that, he investigated a novel process for dry fiber architectures for manufacturing textile pre-forms for ductile composites during his Ph.D. at the University of Manchester. He has ≈ 20 years of experience in Universities and companies related to polymer science, textile technology, 2D materials, and composites.



Shaila Afroj is Senior Research Fellow at the Centre for Print Research (CFPR), UWE Bristol, where she investigates graphene and other 2D materials-based technologies aimed at developing next-generation wearable electronics textiles and sustainable functional clothing. Prior to that, she worked as a Research Associate at the National Graphene Institute, the University of Manchester after completing her Ph.D. from the same university. She has ≈ 14 years of industry (including multi-national companies like C&A and Intertek) and academic experience related to smart textiles, advanced materials, wearable electronics, and fashion textiles.



Kostya S. Novoselov is a condensed matter physicist, specializing in the area of mesoscopic physics and nanotechnology. He is currently Tan Chin Tuan Centennial Professor at the National University of Singapore with broad research interests from mesoscopic transport, ferromagnetism, and superconductivity to electronic and optical properties of graphene and 2D materials. He also has got a vast background in nanofabrication and nanotechnology.



Nazmul Karim is Associate Professor at the Centre for Print Research (CFPR), UWE Bristol. He is currently leading a research team to investigate graphene and other 2D materials-based technologies for developing next-generation wearable electronic textiles, environmentally sustainable functional clothing, and fiber-reinforced smart composites. Prior to that, Karim was a Knowledge Exchange Fellow (graphene) at the National Graphene Institute of the University of Manchester. He has ≈ 14 years of industry and academic experience in new materials and textile-related technologies, and a passion for getting research out of the lab and into real-world applications.